Anonymous Referee #1

We thank the referee for the constructive comments on our manuscript. The referee's comments are given below, followed by our responses.

This manuscript presents an evaluation of the Community Multiscale Air Quality Model (CMAQ) v5.0 against a unique set of size resolved measurements of inorganic aerosol mass.

Similar CMAQ evaluation studies have been published before (as referenced properly), but the present study is the most comprehensive analysis using, as the authors claim, the most extensive data set of size resolved inorganic particle mass available in North America. This data set consists of Micro-orifice Uniform Deposit Impactor (MOUDI) measurements from a rather large number of campaigns conducted across the United States and Canada between the years 2001-2005. This paper is an excellent example that the best observation data available for model evaluation are not necessarily the most recent ones and that it may be very useful to revisit some of the more ancient data sets.

The publication is very well written, clearly structured, and to the point. The analysis is highly relevant as the inorganic fraction makes up a significant fraction of the aerosol, and is fairly unique as model evaluation studies of size-resolved inorganic particle composition are still very scarce. I thus strongly recommend this manuscript for publication in GMD once the following points (mostly minor) have been addressed.

Main point:
Model-observation differences are only discussed in terms of possible model deficiencies implicitly assuming that the measurements are correct. Since I don't know the MOUDI instrument, I cannot really judge the quality of the measurements, but offline aerosol composition measurements may easily be susceptible to sampling biases for some compounds, most notably nitrate. Possible biases of the measurements should be discussed and, if relevant, better emphasized in the manuscript. As explained by the authors, the gas-particle partitioning of nitrate is thermodynamically driven and is a function of temperature and humidity. At what temperatures and humidity are the MOUDI instruments operated? How are the samples treated after collection? PM10 filter samples taken in winter, for example, are known to lose some of the nitrate mass once taken to the lab where they are analyzed at higher temperatures (references xxx). Potential biases in nitrate would also affect the chloride measurements.

In any case, some discussion of measurement uncertainty is needed.

MOUDI instruments are operated at ambient conditions. Particles are collected on filters used as impaction substrates, which are brought back to the laboratory, where they are extracted with deionized water and analyzed by ion chromatography. The referee is correct that nitrate (and to a lesser extent chloride) can be lost by volatilization from filters during sampling.

In the case of the MOUDI measurements made by Colorado State University, parallel measurements of $PM_{2.5}$ nitrate were made using denuder/filter pack sampling trains designed to account for ammonium nitrate volatilization. These measurements show some MOUDI loss of nitrate at most sites, but typically less than 20-30%. This loss is mentioned briefly in the Lee et al. (2008a) paper, but is quantified only in Taehyoung Lee's Ph.D. dissertation. We expect that the degree of volatilization would be similar in the other data sets.

We have changed the last sentence of Section 3.2 to read "The PILS data further demonstrate that aerosol concentrations varied substantially on much shorter timescales than could be captured by the integrated MOUDI measurements, which are subject to volatilization losses during sampling, particularly in summer

(Lee, 2007; Lee et al., 2008a)." In addition, we added two sentences in Section 3.4: "NO_3^- is also subject to measurement artifacts, including the loss of semivolatile ammonium nitrate from the MOUDI. Parallel measurements made using denuder/filter-pack sampling trains designed to account for ammonium nitrate volatilization showed some loss of nitrate at most sites, but typically less than 20-30% (Lee, 2007)."

Minor points:
- Page 3864, line 5: These are "numerical" rather than "mathematical" models

The suggested modification has been made.

- P3866, L13: Since this manuscript evaluates aerosol size distributions and composition, it would be useful to add 2 or 3 sentences here briefly explaining the aerosol module AERO6 (Modal or sectional, number of modes, etc.). This is described later under "Data pairing and analysis" but I feel that section 2.1 would be the better location.

To address this comment, as well as a similar comment by Referee #2, we have revised the text to describe in section 2.1 the version of the CMAQ aerosol model used in the present study:

> The CMAQ model configuration was the same for all simulations, with the only differences being in the year-specific emission and meteorological input data. Aerosols in CMAQ are represented using three lognormal modes—Aitken, accumulation, and coarse (Binkowski and Roselle, 2003). Inorganic species in the Aitken and accumulation modes are assumed to be in thermodynamic equilibrium with the gas phase, while gas-particle partitioning between the gas phase and the coarse mode is treated dynamically (Kelly et al., 2010). The secondary organic aerosol formulation in CMAQ has been described by Carlton et al. (2010). The simulations in this study used CMAQ version 5.0.1 with the AERO6 aerosol module, which includes speciation of trace metals (Reff et al., 2009; Appel et al., 2013) and source-specific ratios of organic mass to organic carbon (Simon and Bhave, 2012), and incorporates version II of the ISORROPIA thermodynamic equilibrium module (Fountoukis and Nenes, 2007).

- P3866, L18: Is this exactly the same 35 layers as in CMAQ? Does CMAQ have a model top at 50 hPa, too?

Yes, these are exactly the same 35 layers. In our runs, WRF and CMAQ had a model top at 50 hPa, but this is configurable. To clarify this is the case, we have reorganized section 2.1 to describe the modeling chain more clearly, first discussing the WRF simulations, including the vertical layering, then MCIP, and finally CMAQ:

> The Weather Research and Forecasting (WRF; Skamarock and Klemp, 2008) model version 3.3 simulated meteorology over the contiguous United States and southern Canada with 12 km by 12 km horizontal grid spacing. A terrain-following sigma vertical coordinate was used, with 35 vertical layers extending up to 50 hPa, and the top of the lowest model layer at approximately 20 m. *[another sentence on WRF configuration]* Version 4.0 of the Meteorology-Chemistry Interface Processor (MCIPv4.0; Otte and Pleim 2010) was used to prepare WRF outputs for CMAQ using the same 35-layer vertical structure as in WRF.

- P3872, L20: How is the model evaluated at mountain sites? At the lowest model level or at the true elevation of the site (which may be well above model ground)? It would be good to add the altitude of the stations in table 1.

WRF uses a terrain-following sigma vertical coordinate, and since here CMAQ is using meteorology fields from WRF, CMAQ inherits this vertical coordinate. Accordingly, the lowest model level is always at the surface, and all sampling locations were in layer 1 of the model. Rather than give the elevation of the stations in Table 1, we have a "Comment" column which we use to describe the terrain (e.g., "clean coastal" or "mountainous". Further details on the sampling locations (including the site elevations) are available in the references given in the right-hand column of Table 1.

- *P3874, L7: I assume you are suspecting that the missing Ca2+ source is sea spray. Why not mention this explicitly?*

We do model Ca^{2+} emissions from sea spray. The higher proportion of Ca^{2+} near the coast is either due to a non-sea-spray origin of Ca^{2+}, or perhaps inaccurate speciation of sea spray (though the latter seems unlikely, given that the chemical composition of seawater is well characterized). We have revised the text to read: "Unlike the situation for Mg^{2+}, the ratio of Ca^{2+} to Na^{+} in the measurements at coastal sites is substantially greater than can be explained by their relative abundances in seawater (Fig. 6 and Supplement Fig. S7). This suggests that there is a source (most likely not originating from seawater) of Ca^{2+} at those sites that is either absent or is underrepresented by the model."

- *P3874, L17ff: Do you know which source of K+ is more important: Natural biomass burning or anthropogenic biofuel burning?*

The answer to this question depends on the specific location and time period of interest, and which class of biomass burning is predominant in that vicinity. While the sources of K^{+} emissions are outside the scope of the present manuscript, we can convey on this Discussion page some information from Reff et al. (2009) who summarized U.S. total emissions for fine-particulate K and other trace elements. During 2002, an estimated 101,000 metric tons of K were emitted to the atmosphere (see Figure S4e of Reff et al.) of which wildfires contributed approximately 14,000 tons. Anthropogenic biofuel burning contributed over 42,000 tons of K, including 33,000 from agricultural burning, 5900 from wood-fired boilers, and 3300 from residential wood combustion. Other large sources of K in the U.S. inventory are agricultural soil (12,000 tons), unpaved road dust (11,000 tons), construction dust (2700 tons), and paved road dust (2300 tons). The U.S. inventory does not include wind-blown dust or sea spray, nor does it separately distinguish K^{+} from total K.

- *P3875, L4: As mentioned earlier, NO3 might not only be a challenge for the model but also for the measurements.*

We have added a sentence noting that semivolatile ammonium nitrate can be lost from MOUDI impaction substrates during sampling, particularly in summer, and that parallel URG denuder/filter-pack measurements at CSU sites quantified the nitrate losses in the MOUDI as typically not more than about 20%.

- *P3877, L5: Could the summer low bias be due to SOA?*

Yes, CMAQ has a negative bias for SOA, which is worst in summer. The text has been modified to insert this point, citing Carlton et al. (2010).

- *P3878: Use past tense as done in section 2.1. Thus, change "are" to "were" on line 2, "is" to "was" on line 9, and "are" to "were" on lines 10 and 12.*

The suggested edits have been made.

- *P3878, L16: "non-carbonaceous organic matter" sounds like a contradiction in itself. Is this supposed to be all molecules other than C?*

The text has been modified to read “noncarbon organic mass (NCOM)” and to cite Simon and Bhave (2012), which describes the use of source-specific organic mass-to-carbon ratios (OM/OC). NCOM is defined as the difference between organic mass (OM) and organic carbon (OC).

- *P3880, L6: PMEMIS should probably be replaced by BASE here.*
No, the CONSIG sensitivity was built on top of PMEMIS. We have deleted “Similar to the PMEMIS sensitivity” from the sentence to clarify.

- *P3881,L27: Again, the obvious reason for the underestimation of Ca2+ at coastal sites is not mentioned explicitly.*

As noted above, the fact that the model does a reasonable job at capturing Na^+ and Mg^{2+} at those sites, but a poor job of capturing Ca^{2+}, suggests that the extra Ca^{2+} is not due to sea spray but rather has some other source, likely windblown dust. We have modified the text to make this point clearer: “By contrast, the model substantially underpredicts Ca^{2+} at many coastal sites while having better performance than for Mg^{2+} at some inland sites, which may be attributable to errors in windblown dust emissions as well as speciation profiles for windblown and anthropogenic fugitive dust.”

- *P3882, L9: Maybe a good place to mention that some of the nitrate biases are related to biases in other ions.*

The fact that nitrate gas-particle partitioning is sensitive to other ions, as well as temperature and humidity, is discussed in Section 3.4. We feel it is not necessary to reiterate that discussion here in the conclusion.

Anonymous Referee #2

We thank the referee for the constructive comments on our manuscript. The referee's comments are noted in italics below, followed by our responses.

General comments:
The current paper compared the simulated size distribution of inorganic aerosol components with the observation in USA and Canada. The evaluation of simulated size distribution is very important for evaluating model performance in simulating impacts of air pollutants on human health and environment. However, long-term and multi-station monitoring of such data is hard to obtain since the MOUDI observation usually needs money and labor. However, the current paper has overcome the limitation by collecting data from the several sets of field campaign across USA and Canada from different years and compared them to one long-term simulation data. The target of the manuscript is well within the scope of the current journal and the manuscript is well written and organized. Therefore, the current manuscript will be accepted after the authors reply to the referee's minor questions and comments, either general or specific, and revise the manuscript, accordingly.

One thing I would like to confirm is about the treatment of hygroscopic growth effects on both measured and simulated aerosol size distribution. My question is at what relative humidity aerosol size distribution was supposed to be measured by the MOUDI system, ambient, room, or even drier than both. Also, is the relative humidity consistent with that used for the derivation of simulated size distribution of chemical components? If the both humidity values are not consistent with each other, it is natural that the measured and simulated size distributions are inconsistent even though the simulation of aerosol size distribution is perfect. Please clarify the humidity measured and used for the calculation.

Because the MOUDI samples are collected at ambient conditions, aerosol water affects particle sizes, and hence on which stages the particles are collected. Aerosol water for all three modes is computed using ISORROPIA II (Fountoukis and Nenes, 2007), which uses Zdanovskii-Stokes-Robinson parameterizations. Aerosol water is included in calculating aerosol modal parameters (i.e., D_g and σ_g), and it is these "wet" diameters and standard deviations that are used in computing the size-composition distributions in the manuscript.

We have modified the text in Section 2.3 to specify that the "wet" modal parameters as output by the CMAQ AERODIAM file are used in the calculations.

Throughout the manuscript, the authors discussed overprediction or underprediction of the peak diameter but it was not clear if the discrepancy is significant or minor. Are there any statistical measures for predictability of peak (or width) of the modeled size distribution?

Whether the discrepancy between observed and modeled size distributions is significant or minor is a good question, but one whose answer depends on what property of the aerosol is of interest for a particular application. Here we focus on $PM_{2.5}$ mass, and devote an entire section of the manuscript (Section 4) to the related question of the difference between estimating $PM_{2.5}$ using the modeled size distribution versus summing the Aitken and accumulation modes, as typically done with CMAQ. As we acknowledge in the conclusion, this evaluation of the modeled size distributions has focused on mass and only on inorganic species. Studies using predictions of carbonaceous size distributions, such as health impacts in urban areas, or studies of the radiative and optical properties of aerosols, might be more sensitive to errors in modeled size distributions.

Specific comments:
[1] p. 3866, ln. 4: "which includes updates to" updates from which version? 5.0.0, or previous?

The text has been revised to remove the ambiguity; see reply to comment [2] below.

[2] p. 3866, ln. 13: "AERO6" needs reference.

There is no single published reference for AERO6. However, to address the referee's comment, as well as a similar comment by Referee #1, we have revised the text to more clearly describe the version of the CMAQ aerosol model used in the present study:

> The CMAQ model configuration was the same for all simulations, with the only differences being in the year-specific emission and meteorological input data. Aerosols in CMAQ are represented using three lognormal modes—Aitken, accumulation, and coarse (Binkowski and Roselle, 2003). Inorganic species in the Aitken and accumulation modes are assumed to be in thermodynamic equilibrium with the gas phase, while gas-particle partitioning between the gas phase and the coarse mode is treated dynamically (Kelly et al., 2010). The secondary organic aerosol formulation in CMAQ has been described by Carlton et al. (2010). The simulations in this study used CMAQ version 5.0.1 with the AERO6 aerosol module, which includes speciation of trace metals (Reff et al., 2009; Appel et al., 2013) and source-specific ratios of organic mass to organic carbon (Simon and Bhave, 2012), and incorporates version II of the ISORROPIA thermodynamic equilibrium module (Fountoukis and Nenes, 2007).

[3] p. 3869, Eq. (2): "Dgv". If Dgv represents geometric volume mean diameter as noted in ln. 21 of p. 3869, √ρj is better to be excluded from Eq. (2). If √ρj is included in Eq. (2), Dgv could be Dgva, e.g. aerodynamic diameter of Dgv, or something like that.

We have modified Eq. (2) to remove the sqrt(ρ_j) and rewritten Eq. (3) so that it is clear that the aerodynamic diameter D_{pa} is the independent variable.

[4] p. 3873, ln. 21-24: "The PILS data … which partially accounts for the scatter in Fig. 5." It is a little bit ambiguous statement. If MOUDI gives accurate average of PILS and the durations of averaging are common for MOUDI and the simulation, the substantial variation of PILS does not account for the scatter in Fig. 5. Or, did you intend to mention the artifact of MOUDI, namely, chemical reactions occurring on the filter during the long duration, whereas PILS gives more accurate values? Please be specific.

The text has been modified to read: "The PILS data further demonstrate that aerosol concentrations varied substantially on much shorter timescales than could be captured by the integrated MOUDI measurements, which are subject to volatilization losses during sampling, particularly during summer (Lee et al., 2008a),

[5] p. 3874, ln. 17-25: How does the model treat K+ emission from biomass burning? Judging from Eq. (6), 0.0176 ACORS could be the one but is it so? ACORS might include anthropogenic and biomass burning and so the factor 0.0176 for biomass burning K+ may vary depending on the relative abundance of anthropogenic versus biomass burning particles in each grid cell. Also ACORS is the coarse mode particles but combustion generated K+ may exist mostly in the fine mode. Does the model consider K+ emission in the fine mode, which is just missing in Eq. (6)?

In AERO6, emissions of K^+ (and other trace metals) in the fine modes are treated explicitly in the model as described in Appel et al. (2013), based on the $PM_{2.5}$ inventory compiled by Reff et al. (2009). The referee is correct that coarse anthropogenic and biomass burning emissions are assigned to the lumped model species ACORS. ACORS is speciated chemically only in computing droplet pH within aqueous chemistry and prior to calling ISORROPIA to compute coarse mode condensation/evaporation. Since biomass burning is predominantly in the submicron mode, its contribution to ACORS is relatively small. We have modified the text to clarify:

> In AERO6, accumulation mode emissions from sea spray are chemically speciated into Na^+, Cl^-, SO_4^{2-}, Mg^{2+}, Ca^{2+}, and K^+ components, but coarse mode sea spray cations are lumped into a single species, ASEACAT, for computational efficiency during transport. Similarly, anthropogenic coarse primary emissions are lumped into ACORS, and coarse windblown soil dust is modeled as ASOIL. Concentrations of individual chemical components in the coarse mode are computed from ASEACAT, ASOIL, and ACORS: *[equations unchanged]*

[6] p. 3875, ln. 17: "the total mass of particles with aerodynamic diameters less than 2.5 μm" Please be a little more specific, e.g. "the total dry mass of particles with ambient aerodynamic diameters less than 2.5 μm". ("50% cut-off diameter is 2.5 μm…" may not be needed here, though.)

The referee has a valid point that filters are equilibrated at a relatively low RH prior to being weighed, so that some aerosol water collected under high humidity is evaporated. However, at least for the U.S. Federal Reference Method for measuring $PM_{2.5}$, particulate water can remain bound to particles even after equilibration, so it is also not correct to say the standard is based only on dry mass. Instead we have modified the text as follows: "In the US, air quality regulations for particulate matter are based on the total mass of particles (after equilibration to room temperature and low humidity) with aerodynamic diameters less than 2.5 μm (Frank, 2006)."

[7] p. 3876, ln. 4: "summer" and "winter" Which months? Please specify.

In general in this paper, "summer" is June, July, and August (JJA); "winter" is December, January, and February (DJF). In this paragraph we are talking about the single year 2002, so "winter" refers to January, February, and December of that year. The text has been revised to clarify this: "The mass-weighted fractions of the accumulation mode and coarse mode in the $PM_{2.5}$ size range averaged over the summer (June-August 2002) and winter (January, February, and December 2002) months are shown in Fig. 8."

[8] p. 3878, ln. 6-7: "implementation of a new gravitational settling scheme". It appears a gravitational settling scheme in a previous version has been updated to a new one. In this case, "implementation of a gravitational settling scheme" would be better.

The text has been modified as suggested.

[9] Table 3: "Dgv" Is it aerodynamic diameter as defined in Eq. (2) or geometric diameter?

It is the geometric volume mean diameter of the mode, consistent with how the term is defined in the text. We have revised Eq. (2) to remove the ambiguity regarding aerodynamic diameter.

[10] Figure 1 (for readers who are not familiar with American geography): The colored circles were hard to be identified. Can those be replaced by numbers or can numbers be added to the colored circles? Also, showing acronyms of sites in the right column of Figure 1 is helpful since only acronyms were used in the main text.

We have modified Figure 1 to replace the site names with the acronyms used in the main text and have changed the symbols to make them larger and more distinguishable. The version of the plot in the discussion paper is from an .eps file, but the resolution seems degraded from the .pdf, which we are providing for the revised manuscript. We are also referencing Table 1 in the caption.

Manuscript prepared for Geosci. Model Dev. Discuss.
with version 2014/09/16 7.15 Copernicus papers of the LaTeX class copernicus.cls.
Date: 29 August 2015

Evaluation of the Community Multiscale Air Quality (CMAQ) model v5.0 against size-resolved measurements of inorganic particle composition across sites in North America

C. G. Nolte[1], K. W. Appel[1], J. T. Kelly[2], P. V. Bhave[3], K. M. Fahey[1], J. L. Collett Jr.[4], L. Zhang[5], and J. O. Young[1]

[1]Atmospheric Modeling and Analysis Division, National Exposure Research Laboratory,
Office of Research and Development, US Environmental Protection Agency,
Research Triangle Park, North Carolina, USA
[2]Air Quality Assessment Division, Office of Air Quality Planning and Standards,
US Environmental Protection Agency, Research Triangle Park, North Carolina, USA
[3]International Centre for Integrated Mountain Development, Kathmandu, Khumaltar,
Lalitpur, Nepal
[4]Department of Atmospheric Science, Colorado State University, Fort Collins, Colorado, USA
[5]Air Quality Research Division, Science and Technology Branch, Environment Canada, Toronto,
Ontario, Canada

Correspondence to: C. G. Nolte (nolte.chris@epa.gov)

Abstract

This work evaluates particle size-composition distributions simulated by the Community Multiscale Air Quality (CMAQ) model using Micro-Orifice Uniform Deposit Impactor (MOUDI) measurements at 18 sites across North America. Size-resolved measurements of particulate SO_4^{2-}, NO_3^-, NH_4^+, Na^+, Cl^-, Mg^{2+}, Ca^{2+} and K^+ are compared to CMAQ model output for discrete sampling periods between 2002 and 2005. The observation sites were predominantly in remote areas (e.g. National Parks) in the United States and Canada, and measurements were typically made for a period of roughly one month. For SO_4^{2-} and NH_4^+, model performance was consistent across the US and Canadian sites, with the model slightly overestimating the peak particle diameter and underestimating the peak particle concentration compared to the observations. Na^+ and Mg^{2+} size distributions were generally well represented at coastal sites, indicating reasonable simulation of emissions from sea spray. CMAQ is able to simulate the displacement of Cl^- in aged sea spray aerosol, though the extent of Cl^- depletion relative to Na^+ is often underpredicted. The model performance for NO_3^- exhibited much more site-to-site variability than that of SO_4^{2-} and NH_4^+, with the model ranging from an underestimation to overestimation of both the peak diameter and peak particle concentration across the sites. Computing $PM_{2.5}$ from the modeled size distribution parameters rather than by summing the masses in the Aitken and accumulation modes resulted in differences in daily averages of up to $1\,\mu g\,m^{-3}$ (10 %), while the difference in seasonal and annual model performance compared to observations from the IMPROVE, CSN and AQS networks was very small. Two updates to the CMAQ aerosol model – changes to the assumed size and mode width of emitted particles and the implementation of gravitational settling – resulted in small improvements in modeled size distributions.

1 Introduction

A detailed understanding of the size, chemical composition, and atmospheric concentration of particulate matter (PM) is needed to assess its effects on human health, visibility, ecosystems, and climate. Assessments of these various PM effects are typically done with ~~mathematical~~ numerical models, and our confidence in the models is established through rigorous evaluation against ambient measurements. The mass concentration, size distribution, and bulk chemical composition of atmospheric PM are most often measured separately, and models are typically evaluated against these independent measures (e.g., Simon et al., 2012). However, it is well established that the PM composition varies considerably with particle size, and these size-resolved chemical characteristics govern the optical and radiative properties of PM. Because the aerodynamic behavior of PM is also a strong function of particle size, the size distributions of different chemical components also influence the human health and environmental effects of PM by affecting where particles deposit in the respiratory tract (Asgharian et al., 2001) or whether they are transported to sensitive ecosystems (Scheffe et al., 2014).

Inertial cascade impactors are the most robust devices for collecting size-resolved ambient particles and analyzing their chemical composition (e.g., Marple et al., 1991). Because operating a cascade impactor is labor-intensive and costly, their use has been restricted historically to field studies at individual locations or multi-site campaigns within small geographic regions (e.g., Herner et al., 2005). Previously, size-composition distributions simulated by the Community Multiscale Air Quality (CMAQ) model were evaluated against Micro-Orifice Uniform Deposit Impactor (MOUDI) measurements of inorganic particle components at three coastal urban sites in Tampa, Florida during May 2002 using CMAQ's standard modal aerosol formulation (Kelly et al., 2010) and a sectional formulation (Nolte et al., 2008). Kelly et al. (2011) evaluated size-composition distributions of inorganic and carbonaceous PM against MOUDI data at five sites in California's Central Valley as well as Bodega Bay and Sequoia during a wintertime episode. Also, Zhang et al. (2006) evaluated CMAQ predictions of total particle volume distributions in Atlanta, and Elleman and Covert (2010) evaluated predictions of total particle mass in two sub-micron size ranges in the Pacific Northwest. These studies indicate that CMAQ often overpredicts the peak diameter of PM mass-size distributions and the widths of the lognormal particle modes. Kelly et al. (2011) reported that in some urban areas (e.g., Fresno, California) CMAQ adequately predicted the observed peak diameter for inorganic components but overpredicted the peak diameter of the organic and elemental carbon distributions. Overpredictions of particle diameter were found to lead to underpredictions of the PM mass in the sub-2.5 µm size range ($PM_{2.5}$).

The scarcity of impactor data has prevented any model evaluation of size-composition distributions across a continental-scale domain. Such an evaluation would enhance our confidence in models for assessing the human health and ecosystem effects of PM. From 2001–2005, a pair of field campaigns was conducted on a large geographic scale to yield size-segregated impactor measurements of the inorganic PM composition at 14 rural sites across the United States and Canada (Zhang et al., 2008; Lee et al., 2008a). In this paper, we evaluate size-composition distributions modeled by CMAQ against impactor measurements collected during these two campaigns, as well as urban-scale campaigns conducted in Pittsburgh and Tampa. We identify the regions and seasons where model performance is best as well as those where further model development is needed. Some implications on future evaluations of CMAQ output against routine measurements of $PM_{2.5}$ composition are also discussed.

2 Data

2.1 ~~CMAQ~~ Model simulations

The measurements used in this study were taken during discrete sampling periods within field campaigns spread across the years 2001–2005; therefore several years of ~~CMAQ~~ model simulations were required in order to create a comprehensive analysis dataset. Four years of ~~CMAQ~~ meteorology and air quality simulations were conducted, covering the period 2002–2005. The ~~CMAQ model configuration was the same for all simulations, with the only differences being in the year-specific emission and meteorological input data. The simulations utilized CMAQ version 5.0.1, which includes updates to the treatment of anthropogenic fugitive dust and windblown dust , as well as bi-directional surface exchange~~

~~. The simulations were performed for a domain covering the~~ Weather Research and Forecasting (WRF; Skamarock and Klemp, 2008) model version 3.3 simulated meteorology over the contiguous United States and southern Canada ~~utilizing~~ with 12 km by 12 km horizontal grid spacing~~and~~. A terrain-following sigma vertical coordinate was used, with 35 vertical layers ~~, with~~ extending up to 50 hPa, and the top of the lowest model layer at approximately 20 m. ~~Lateral boundary conditions (BCs) for the CMAQ simulations were obtained from monthly median concentrations from a GEOS-Chem model simulation of the year 2005 (the same BCs were used for all four years) using the procedure described by . Other model options employed include the AERO6 aerosol module, the Carbon Bond chemical mechanism that includes toluene and chlorine chemistry , and online computation of photolysis rates.~~

~~Meteorological data were provided from Weather Research and Forecast model version 3.3 simulations of 2002–2005. The WRF model~~ The WRF simulations were performed using ~~35 vertical layers extending up to 50,~~ the Pleim-Xiu land-surface model (PX-LSM; Pleim and Xiu, 1995), the ACM2 planetary boundary layer (PBL) scheme (Pleim, 2007a, b), the Kain-Fritsch cumulus parameterization scheme (Kain, 2004), the Morrison microphysics scheme (Morrison et al., 2009) and four-dimensional data assimilation with no nudging in the PBL. Version 4.0 of the ~~Meteorology Chemistry~~ Meteorology-Chemistry Interface Processor (MCIPv4.0; Otte and Pleim, 2010) was used to prepare WRF outputs for CMAQ using the same 35-layer vertical structure as in WRF.

The CMAQ model configuration was the same for all simulations, with the only differences being in the year-specific emission and meteorological input data. Aerosols in CMAQ are represented using three lognormal modes–Aitken, accumulation, and coarse (Binkowski and Roselle, 2003). Inorganic species in the Aitken and accumulation modes are assumed to be in thermodynamic equilibrium with the gas phase, while gas-particle partitioning between the gas phase and the coarse mode is treated dynamically (Kelly et al., 2010). The secondary organic aerosol formulation in CMAQ has been described by Carlton et al. (2010). The simulations in this study used CMAQ version 5.0.1 with the AERO6 aerosol module, which includes speciation of trace metals (Reff et al., 2009; Appel et al.,

2013) and source-specific ratios of organic mass to organic carbon (Simon and Bhave, 2012), and incorporates version II of the ISORROPIA thermodynamic equilibrium module (Fountoukis and Nenes, 2007). Other CMAQ model options employed include online computation of photolysis rates (Foley et al., 2010), a Carbon Bond chemical mechanism modified to include toluene and chlorine chemistry (CB05TUCL; Sarwar et al., 2011), and NH_3 bi-directional surface exchange (Bash et al., 2013). Lateral boundary conditions (BCs) for the CMAQ simulations were obtained from monthly median concentrations from a GEOS-Chem (Bey et al., 2001) model simulation of the year 2005 (the same BCs were used for all four years) using the procedure described by Henderson et al. (2014).

Hourly, gridded emission data from non-mobile sources between 2002–2005 were created using version 3.1 of the Sparse Matrix Operator Kernel Emissions (SMOKEv3.1; Houyoux et al., 2000) model and are based on the 2002 National Emissions Inventory (NEI) for the years 2002–2004 (2003 and 2004 are projected from 2002) and the 2005 NEI for 2005. Continuous emission monitoring (CEM) data were used for the electric generating units sector. Wildfire emissions were based on daily fire detections from the Hazard Mapping System and the Sonoma Technology SMARTFIRE system ~~()~~(Raffuse et al., 2009).

Hourly mobile emissions were created using year-specific traffic and meteorological data in version 2010b of the Motor Vehicle Emission Simulator (MOVESv2010b; http://www.epa.gov/otaq/models/moves). $PM_{2.5}$ emissions of eight trace metals, including Mg^{2+}, Ca^{2+}, and K^{+}, were speciated using the profiles in Reff et al. (2009). Other model configuration options affecting emissions include online emissions of accumulation and coarse mode Na^{+}, Cl^{-}, SO_4^{2-}, Mg^{2+}, Ca^{2+}, and K^{+} from sea spray (Kelly et al., 2010), online NO emissions using lightning flash counts from the National Lightning Detection Network (NLDN; Allen et al., 2012); BELD3 land-use for gridded fractional crop distributions; version 3.1.4 of the Biogenic Emissions Inventory System (BEIS v3.1.4; Vukovich and Pierce, 2002) for online biogenic emissions; the 2001 version of the National Land Characterization Database (NLCD) for land-use data; and NH_3 emissions from fertilizer based on an Environmental Policy Integrated Climate (EPIC; Cooter et al., 2012) simulation using 2002 fertilizer sales data.

2.2 MOUDI measurements

The MOUDI measurements used in this study are from four distinct datasets, with one dataset consisting of observations from wilderness sites located in several Canadian provinces (Zhang et al., 2008), another set consisting of sites primarily located in US National Parks (Malm et al., 2005; Lee et al., 2008a), a smaller dataset from sites available during the Bay Region Atmospheric Chemistry (BRACE) study in Tampa, Florida (Evans et al., 2004), and finally a dataset collected during the Pittsburgh Air Quality Study (Cabada et al., 2004). Data are available from 18 distinct sites covering 24 observation periods generally ranging in length from two to four weeks and covering each season of the year. To our knowledge, this collection represents the most comprehensive dataset collected to date characterizing inorganic PM size-composition distributions for multiple locations across the US and Canada and under diverse meteorological conditions. A brief description of the MOUDI data is provided below and a summary of the site locations and observation dates is provided in Table 1, with locations illustrated in Fig. 1.

Aerosol ion (SO_4^{2-}, NO_3^-, NH_4^+, Cl^-, Na^+, Mg^{2+}, Ca^{2+} and K^+) size distributions were measured at eight Canadian sites (i.e. ALG, BRL, CHA, EGB, FRS, KEJ, LED and SPR) (Zhang et al., 2008). The number of samples and the sample duration varied among monitors, with 7 being the fewest and 24 being the most samples taken during any one observation period, while the shortest sample duration was 6 h and the longest 152 h. Standard ion chromatography was used for analyses of all filters after extraction in deionized water. Additional details regarding these measurements can be found in Zhang et al. (2008).

Size distributions of the same particle ions were collected at the BON, SGO, GRC, GSM, YOS and BRG sites in the US. To ensure adequate mass collection at these rural locations, samples were typically collected over a 48 h period, with the exception of Yosemite ~~NP~~ which used 24 h sampling periods. A total of seven study periods are available from these sites in 2002–2004, with one study period in 2002 from mid-July through mid-August (YOS), five study periods in 2003 occurring in February (BON), April (SGO1), May (GRC), July (SGO2) and November (BRG), and one study period in 2004 from mid-July through mid-August (GSM). Additional details regarding these data can be found in Lee et al. (2008a).

Aerosol ion size distributions in three urban locations were collected during the BRACE study in Florida in 2002 at the AZP, GAN and SYD sites and in PIT in January 2002 (Table 1). Similar to the other two datasets described above, the BRACE data were collected using MOUDI samplers with 8 or 10 fractionation stages, an inlet height of 2 m, and a flow rate of 30 L min^{-1} for sample durations of approximately 23 h. Samples were collected on 15 days at the AZP and GAN sites and 14 days at the SYD site between 4 May and 2 June for a total of 58 samples. Samples at the Pittsburgh site were collected during 1–17 January for a total of 11 samples. Additional details regarding the BRACE data can be found in Evans et al. (2004) and Nolte et al. (2008), while additional details on the Pittsburgh data can be found in Cabada et al. (2004) and Stanier et al. (2004).

2.3 Data pairing and analysis

The particle size distribution data consist of multiple measurements taken over a period of several weeks. Since the analysis is focused on broad persistent features rather than day-to-day variability, the data here are averaged into a single observed and modeled size distribution for each ion for each campaign listed in Table 1, where the model output is averaged over the days and times corresponding to each sampling period. The CMAQ aerosol model uses three lognormal modes (Aitken, accumulation, and coarse) to represent particle size distributions (Binkowski and Roselle, 2003), whereas the observations are separated into discrete size bins. To facilitate comparison between the model and the observations, the three modes in the model are summed to produce a single smooth curve. For each mode j, mass concentrations $M_j = \sum\limits_i M_{ij}$ are obtained from the CMAQ hourly average concentration (ACONC) files, where M_{ij} is the mass of constituent i in mode j. ~~Modal~~ “Wet” (i.e., including aerosol water) modal parameters $D_{\mathrm{g},j}$, $\sigma_{\mathrm{g},j}$, and $M_{3,j}$ are taken from the aerosol diagnostic (AERODIAM) output files, where $D_{\mathrm{g},j}$ is the geometric number mean diameter of mode j, $\sigma_{\mathrm{g},j}$ is the geometric standard deviation of mode j, and $M_{3,j}$ is the third moment of mode j. Particle densities ρ_j ($\mathrm{g\,cm^{-3}}$) are calculated as

$$\rho_j = \frac{10^{-12}}{M_{3,j}} \frac{6}{\pi} M_j . \tag{1}$$

The geometric volume mean diameters D_{gv} are calculated from the number mean diameters using the Hatch–Choate relation

$$D_{\mathrm{gv},j} = D_{\mathrm{g},j} \underline{\sqrt{\rho_j}} \exp\left(3 \ln^2 \sigma_{\mathrm{g},j}\right) . \tag{2}$$

~~where the multiplication by $\sqrt{\rho_j}$ puts the expression in terms of the particle aerodynamic diameter for consistency with the measurements.~~ The size distribution at each hour t is then computed as

$$\underline{\frac{\mathrm{d}M}{\mathrm{d}\ln D_p}} (D_p \frac{\mathrm{d}M}{\mathrm{d}\ln D_{pa}} (D_{pa}, t) = \sum_{j=1}^{3} \frac{M_j}{\sqrt{2\pi} \ln \sigma_{\mathrm{g},j}} \exp \underline{\frac{-(\ln D_p - \ln D_{\mathrm{gv},j})^2}{2 \ln^2 \sigma_{\mathrm{g},j}}} \frac{-(\ln D_{pa} - \frac{1}{2} \ln \rho_j - \ln D_{\mathrm{gv},j}}{2 \ln^2 \sigma_{\mathrm{g},j}} \tag{3}$$

where the $\frac{1}{2} \ln \rho_j$ term accounts for using the aerodynamic diameter D_{pa} as the independent variable, to facilitate comparison with measured size distributions. The above equation is discretized by ~~$\ln D_p$~~$\ln D_{pa}$, and the discretized values are computed for each hour before finally computing the temporally averaged size distribution.

For Aitken and accumulation mode species, the inputs to Eq. (3) are obtained directly from CMAQ outputs for the corresponding grid cell, but directly emitted coarse mode species require special processing. In ~~CMAQ v5.0~~AERO6, accumulation mode emissions from sea spray are chemically speciated into $\mathrm{Na^+}$, $\mathrm{Cl^-}$, $\mathrm{SO_4^{2-}}$, $\mathrm{Mg^{2+}}$, $\mathrm{Ca^{2+}}$, and $\mathrm{K^+}$ components, but coarse mode sea spray cations are lumped into a single species, ASEACAT, for computational efficiency during ~~advection.~~ transport. Similarly, anthropogenic coarse primary emissions are lumped into ACORS, and coarse windblown soil dust is modeled as

ASOIL. Concentrations of individual chemical components in the coarse mode are computed from ASEACAT, ~~soil dust (~~ASOIL~~), and coarse primary emissions (~~, and ACORS~~)~~:

$$\mathrm{ANAK} = 0.8373 \cdot \mathrm{ASEACAT} + 0.0626 \cdot \mathrm{ASOIL} + 0.0023 \cdot \mathrm{ACORS} \tag{4}$$

$$\mathrm{AMGK} = 0.0997 \cdot \mathrm{ASEACAT} + 0.0032 \cdot \mathrm{ACORS} \tag{5}$$

$$\mathrm{AKK} = 0.0310 \cdot \mathrm{ASEACAT} + 0.0242 \cdot \mathrm{ASOIL} + 0.0176 \cdot \mathrm{ACORS} \tag{6}$$

$$\mathrm{ACAK} = 0.0320 \cdot \mathrm{ASEACAT} + 0.0838 \cdot \mathrm{ASOIL} + 0.0562 \cdot \mathrm{ACORS} \tag{7}$$

In Equations (4)–(7), ANAK, AMGK, AKK, and ACAK are coarse mode Na^{+}, Mg^{2+}, K^{+}, and Ca^{2+}, respectively, and the coefficients are relative abundances in seawater and composite weighting factors based on profiles in the SPECIATE database (Simon et al., 2010).

3 Evaluation of size distributions

In this section CMAQ modeled size-composition distributions are compared to the MOUDI measurements. For brevity, a few representative sites and time periods are presented for each ion. Plots of the average modeled and measured size distributions for all 24 campaigns listed in Table 1 are available in the Supplement for each of the inorganic ions analyzed.

3.1 SO_4^{2-} and NH_4^{+}

Modeled and observed SO_4^{2-} size distributions at each site and averaged over each sampling campaign are shown in Supplement Fig. S1. The model generally captures the variability in the SO_4^{2-} size distribution across different sites and different seasons. As shown in Fig. 2, the model accurately reproduces the observed SO_4^{2-} size distribution at many sites, including LED2, SPR2, SGO1, and SYD. However, the model fails to capture the accumulation mode peak observed in many of the campaigns (e.g., ALG1 and GSM), and often the modeled peak diameter is shifted to larger sizes (e.g., BRL and CHA2) than indicated by the measurements.

The model performance for particle NH_4^+ (Fig. 3 and Supplement Fig. S2) generally follows that of SO_4^{2-}, with the model tending to underestimate the accumulation mode peak concentration and overestimating the aerodynamic diameter where the peak occurs. Modeled and observed NH_4^+ size distributions are generally in good agreement at those sites where SO_4^{2-} performance is best (i.e., LED2, SPR2, and SYD), though there is a large NH_4^+ underprediction at SGO1 in contrast to good SO_4^{2-} performance there. This behavior is consistent with recent studies that have reported that NH_3 emissions in southern California's South Coast Air Basin are underestimated in the NEI (Nowak et al., 2012; Kelly et al., 2014). Similarly to the performance for SO_4^{2-}, the model largely underestimates the NH_4^+ accumulation mode peak and overestimates the diameter at which the peak occurs at ALG1, GSM, BRL, and CHA2.

3.2 Na^+ and Cl^-

Sea spray is the principal source of Na^+ and, at most locations, the dominant source of Cl^- as well. Average modeled and observed Na^+ size distributions are plotted for the coastal and near-coastal sites in Fig. 4. Cl^- size distributions generally follow those for Na^+ and accordingly they are not further discussed here, though Na^+ and Cl^- plots across all the campaigns are presented in Supplement Figs. S3 and S4. CMAQ generally captures the Na^+ size distributions and elevated concentrations at the coastal sites, i.e., the BRACE sites (AZP, GAN, and SYD), as well as BRG and KEJ. At most of the other sites, Na^+ concentrations are very low; often concentrations at these sites are near the detection limit, and confidence in the measurements is relatively low (Zhang et al., 2008). CMAQ correctly simulates that Na^+ concentrations are low at these low-concentration sites, though size distributions do not agree very well with measurements (Supplement Fig. S3). The ALG site near Lake Superior is not impacted by sea spray; the relatively high Na^+ concentrations in ALG1 are due to the application of salt to roads to prevent ice formation during the winter (Zhang et al., 2008). As this Canadian road salt is not in the US NEI, it is not surprising that the model is unable to capture this peak. SGO is in a mountainous wilderness area about 100 km from the Pacific Ocean. Because simulating winds over mountainous terrain is challenging, particularly with 12 km grid cells, CMAQ's relatively poor performance for Na^+ at SGO2 is likely attributable to errors in transport to the SGO site.

The concentration of Cl^- in fresh sea spray aerosol is proportional to its abundance in seawater. While Na^+ and other sea salt cations are chemically inert, under certain conditions Cl^- in aged sea spray particles can be displaced by condensed gas-phase acids, such as HNO_3. The percentage of chloride depleted can be defined as (Yao and Zhang, 2012)

$$\mathrm{Cl}^-_{\mathrm{depletion}}(\%) = \frac{\alpha[\mathrm{Na}^+] - [\mathrm{Cl}^-]}{\alpha[\mathrm{Na}^+]} \cdot 100 \tag{8}$$

where $[Na^+]$ and $[Cl^-]$ are molar equivalent concentrations and α is the ratio of the relative molar abundance of Cl^- to Na^+ in seawater, equal to 1.164 in CMAQ. The modeled percentages of chloride depletion are compared to the individual measurements at near-coastal sites in Fig. 5. Consistent with previous results of Kelly et al. (2010), the model frequently underestimates the moderate (25–50 %) levels of chloride depletion seen at the BRACE sites (AZP, GAN, and SYD), which are within 20 km or less from Tampa Bay. The negative bias in the amount of chloride depletion is slightly greater at BRG (not shown). For the rural coastal KEJ site in Nova Scotia, the model slightly underestimates the chloride depletion during the fall campaign (KEJ2), but severely underestimates the frequently near-total depletion observed during the summer (KEJ1) (Yao and Zhang, 2012). For the springtime campaign SGO1, the modeled Cl^- depletion is overestimated. There are significant contributions of sodium from the primary species ASOIL and ACORS for SGO1, which could be contributing to an overprediction of Na^+ and hence an overprediction of Cl^- depletion. For the summer SGO2 campaign, the model correctly simulates chloride depletions approaching 100 %, while at YOS the modeled degree of chloride depletion is sometimes greater than observed. Highly time-resolved measurements were made using a Particle-Into-Liquid Sampler (PILS) at the same locations and times as the MOUDI measurements that are the focus of this study (Lee et al., 2008b). The PILS measurements show that NO_3^- peaks coincide with Cl^- dropping below detection limits at YOS and SGO2, providing strong evidence of chloride displacement from condensation of HNO_3. The PILS data further demonstrate that aerosol concentrations varied substantially on much shorter timescales than could be captured by the integrated MOUDI measurements, which ~~partially accounts for the scatter in Fig. 5.~~ are subject to volatilization losses during sampling, particularly in summer (Lee, 2007; Lee et al., 2008a).

3.3 Mg^{2+}, Ca^{2+} and K^+

At coastal sites, modeled Mg^{2+} concentrations generally follow modeled Na^+ concentrations in accordance with their relative abundances in seawater, and model performance for Mg^{2+} generally follows that for Na^+ at these sites. At AZP (Fig. 6) as well as GAN, SYD, BRG, KEJ1, KEJ2, ALG1, and SGO2 (Supplement Fig. S6), the observed and modeled Mg^{2+} size distributions have the same relationship to each other as the corresponding Na^+ size distributions at those sites. At BRL, GRC, and YOS, Mg^{2+} is likely to have a crustal rather than oceanic origin. At these western sites, Mg^{2+} is underpredicted (Fig. 6), consistent with findings of Appel et al. (2013). Unlike the ~~behavior~~ situation for Mg^{2+}, ~~modeled~~ the ratio of Ca^{2+} ~~is notably underpredicted~~ to Na^+ in the measurements at coastal sites is substantially greater than can be explained by their relative abundances in seawater (Fig. 6 and Supplement Fig. S7). This suggests that there is a source (most likely not originating from seawater) of Ca^{2+} at those sites ~~not captured~~ that is either absent or is underrepresented by the model. On the other hand, modeled Ca^{2+} is higher than modeled Mg^{2+} at BRL, GRC, and YOS, in better agreement with observations, indicating that the coarse mode Ca^{2+} at those sites is due to contributions from anthropogenic fugitive dust or soils rather than sea spray. The chemical speciation of windblown dust and directly emitted coarse PM is derived from four California desert soil profiles in SPECIATE. Because these profiles did not report Mg, these sources do not contribute to Mg^{2+} concentrations modeled by CMAQ. The relatively good model performance for Ca^{2+} and underprediction of Mg^{2+} at these sites suggest that the Mg^{2+} speciation factors for primary coarse PM and windblown dust should be revisited.

Model performance for K^+ is notably better than for Ca^{2+}, with the model reasonably capturing the observed pattern at most sites (Fig. 6 and Supplement Fig. S7). K^+ is known to be emitted from biomass burning in addition to the sea spray and dust sources that also impact Ca^{2+}. The impact of the combustion source of K^+ is evident in the smaller peak diameters for the K^+ than the Mg^{2+} and Ca^{2+} observed distributions. The model simulates a bimodal distribution at GRC where the observed distribution was a broad single mode, and the coarse mode is underpredicted at YOS. Overall however, the model does well in simulating the observed K^+ particle distribution at the majority of the Canadian and US sites.

3.4 NO_3^-

Aerosol NO_3^- is formed almost entirely from condensation of gas-phase HNO_3 on existing particles. Moreover, the degree of gas-particle mass transfer for nitrate is thermodynamically driven, and is a strong function of inorganic particle composition as well as temperature and relative humidity. As a result, the NO_3^- size distribution depends on the distribution of other ions, especially SO_4^{2-} and NH_4^+, making it particularly challenging to model accurately (Yu et al., 2005). NO_3^- is also subject to measurement artifacts, including the loss of semivolatile ammonium nitrate from the MOUDI. Parallel measurements of $PM_{2.5}$ nitrate made using denuder/filter-pack sampling trains designed to account for ammonium nitrate volatilization showed some loss of nitrate at most sites, but typically less than 20–30% (Lee, 2007).

Model performance for NO_3^- (Fig. 7 and Supplement Fig. S8) ~~. Model performance for~~ is generally good at ALG1, CHA1, and KEJ1, though the coarse mode is somewhat underpredicted at these sites, while the accumulation mode is slightly overpredicted at LED2. Despite the greater surface area of the fine modes, NO_3^- often resides in the coarse mode when the fine modes are too acidic from condensation of H_2SO_4, which has lower vapor pressure than HNO_3 under ambient conditions. At BRL and BON, the modeled size distribution is broader and shifted slightly to larger particles than measured by the MOUDI. At SGO1 and YOS, particle NO_3^- is significantly underestimated. These errors in modeled

NO_3^- concentrations can be attributed to underestimated levels of accumulation-mode NH_4^+ at SGO1 and underestimated coarse-mode Na^+ at YOS (cf. Fig. 7 and Supplement Fig. S3).

4 Modeled PM$_{2.5}$

In the US~~as well as many other countries~~, air quality regulations for particulate matter are based on the total mass of particles (after equilibration to room temperature and low humidity) with aerodynamic diameters less than 2.5 ~~()~~µm Frank (2006). Most CMAQ model evaluations, however (e.g., Appel et al., 2008), have used the sum of PM in the Aitken (i) and accumulation (j) modes (i.e. PM$_{ij}$), to represent PM$_{2.5}$. As noted by Jiang et al. (2006), PM$_{ij}$ and PM$_{2.5}$ are conceptually distinct quantities that sometimes differ significantly. Since the release of CMAQ v4.5 in 2005, additional variables are output to an optional diagnostic file (i.e., AERODIAM) that facilitate a more rigorous calculation of modeled PM$_{2.5}$ based on the simulated size distribution. Despite this capability, PM$_{ij}$ is still typically used for CMAQ model evaluation (Foley et al., 2010). As a further evaluation of CMAQ modeled aerosol size distributions, here we compare modeled PM$_{2.5}$ to the traditional PM$_{ij}$ calculations and to observed total PM$_{2.5}$ from the IMPROVE, CSN and AQS networks for 2002.

The mass-weighted fractions of the accumulation mode and coarse mode in the PM$_{2.5}$ size range averaged over the summer ~~and winter seasons~~ (June–August 2002) and winter (January, February, and December 2002) months are shown in Fig. 8. Although during the winter the vast majority of the accumulation mode is smaller than 2.5 µm, during the summer up to 10–12 % of the accumulation mode is greater than 2.5 µm in size. The smaller fraction of the accumulation mode in the PM$_{2.5}$ size range in the eastern US is attributable to larger amounts of aerosol water, both because of higher humidities and higher concentrations of hygroscopic SO_4^{2-}. The fractional contribution of the coarse mode to PM$_{2.5}$ is fairly uniform, ranging from 10–15 %, though there are a few areas where the contribution exceeds 20 %. Modeled PM$_{2.5}$ is 0.3–1.2 µg m^{-3} lower than PM$_{ij}$ across a large portion of the eastern US during the summer (Fig. 9), primarily due to the greater contributions of SO_4^{2-}, NO_3^-, NH_4^+ and EC to PM$_{ij}$ than PM$_{2.5}$ concentrations. In the western US, PM$_{2.5}$ values are sporadically higher (primarily in Texas, New Mexico, Arizona and southern California) due almost exclusively to the greater contributions of soil (i.e. Al, Si, Ca, Fe and Ti) to $PM_{2.5}$ than PM_{ij} that result from the tail of the coarse mode overlapping the $PM_{2.5}$ size range. The relative differences are 4–12 % in the eastern US during summer and 4–20 % in the western US (Supplement Fig. S9).

Histograms of the difference in CMAQ daily mean aerosol concentrations (modeled $PM_{2.5}$ − modeled PM_{ij}) at IMPROVE, CSN and AQS-FRM sites for 2002 are also shown in Fig. 9. The distribution of mean differences is predominantly negative, particularly during summer and fall (not shown), indicating that PM_{ij} is generally greater than $PM_{2.5}$. For all seasons, the differences in $PM_{2.5}$ and PM_{ij} typically fall between ±1 µg m^{-3}.

The mean bias (MB), mean error (ME) and root mean square error (RMSE) as computed against the IMPROVE, CSN and AQS-FRM observations using modeled $PM_{2.5}$ and PM_{ij} values are provided in Table 2. The difference in network- and seasonally-averaged MB, ME, and RMSE computed using $PM_{2.5}$ and PM_{ij} is generally small. For winter, spring, and fall, average $PM_{2.5}$ is 0.04–0.20 µg m^{-3} less than PM_{ij}. Since the model is generally positively biased with respect to observations during those seasons, using $PM_{2.5}$ rather than PM_{ij} results in slightly improved performance statistics. The difference between $PM_{2.5}$ and PM_{ij} is larger (more negative) during the summer~~, and since~~. Since the model is generally negatively biased ~~then,~~ during the summer, largely due to underpredictions of secondary organic aerosol (Carlton et al., 2010), the MB, ME, and RMSE are all slightly worse for $PM_{2.5}$ than for PM_{ij}. The differences during the summer are still small, however, averaging 0.30 µg m^{-3} for MB, 0.22 µg m^{-3} for ME, and 0.21 µg m^{-3} for RMSE. Overall, the aggregated model performance using modeled $PM_{2.5}$ and PM_{ij} is nearly the same, with the average difference ($PM_{2.5} - PM_{ij}$) in MB, ME and RMSE across all seasons of −0.15, 0.02 and 0.02 µg m^{-3}, respectively. Therefore, while the difference between $PM_{2.5}$ and PM_{ij} values for any particular observation site and time may be important, the difference in model performance between the two values is relatively small on average. The difference in the two methods for estimating $PM_{2.5}$ is likely to be even smaller when the models are applied in a relative sense for a regulatory context (Baker and Foley, 2011).

In the version of CMAQ (v4.3) used by Jiang et al. (2006), there was very little mass in the coarse mode, and this mode was modeled as being chemically inert. Thus, PM_{ij} was always greater than $\mathrm{PM}_{2.5}$ in that version. Because the model was generally positively biased with respect to measurements, using the size distribution to compute $\mathrm{PM}_{2.5}$ improved model performance statistics. There have been several updates to the CMAQ aerosol model since the version used by Jiang et al. (2006). For this discussion, the most significant of these are the reduction of overestimated unspeciated $\mathrm{PM}_{2.5}$ (i.e., PMOTHER; Appel et al., 2008, 2013; Foley et al., 2010), and the treatment of gas-particle nitrate mass transfer to and from coarse mode particles (Kelly et al., 2010). As a result, the consequence of estimating $\mathrm{PM}_{2.5}$ concentrations by using the modeled size distributions rather than by summing the masses in the Aitken and accumulation modes has been changed such that ~~it~~ doing so does not always improve model performance.

5 Model sensitivities

Four additional simulations ~~are~~ were conducted to assess the sensitivity of modeled size distributions to changes in the aerosol model. The "BASE" model configuration used for the sensitivity runs ~~contains~~ contained various updates from CMAQ v5.0.1, but overall results of the BASE simulation used for these sensitivity studies ~~are~~ were very similar to those presented in Sect. 3. The three sensitivity studies ~~include~~ included an adjustment to the apportionment of PM emissions between modes and the implementation of a ~~new~~ gravitational settling scheme, two changes that are planned to be included in CMAQ v5.1 (scheduled for release in fall 2015). In addition, a third simulation ~~is~~ was performed where the allowable particle mode widths (i.e. geometric standard deviations) in the model are constrained to a relatively narrow range. The details of each sensitivity analysis are described in the following three sub-sections. The sensitivity tests ~~are~~ were each performed for May 2002 and compared to data from the three BRACE sites in Tampa during that month.

5.1 PM emissions adjustment

~~Currently (i.e., in~~ In CMAQ v5.0.2~~)~~, primary anthropogenic emissions of $PM_{2.5}$ elemental carbon (EC), organic carbon (OC), and ~~non-carbonaceous organic matter (NCOM)~~ noncarbon organic mass (NCOM; Simon and Bhave, 2012) are mostly (99.9 %) assigned to CMAQ's accumulation mode, with the remaining 0.1 % assigned to the Aitken mode. Primary anthropogenic emissions of other species (i.e., sulfate, nitrate, chloride, ammonium, sodium, water, and "other") are 100 % assigned to the accumulation mode. As noted by Elleman and Covert (2010), these modal mass fractions are based on historical measurements that underestimated ultrafine particles. In an effort to improve simulation of aerosol number size distributions, Elleman and Covert (2010) updated particulate emissions size distributions based on a review of modern measurements in regions dominated by urban, power-plant, and marine sources at 4–15 km spatial scales. In the "PMEMIS" sensitivity test, the modal mass fractions for "urban" PM emissions from Elleman and Covert (2010) (i.e., 10 % Aitken mode, 90 % accumulation mode) were applied to all primary anthropogenic $PM_{2.5}$ emissions. In addition, the modal parameters characterizing the emitted particles (i.e., geometric mean volume diameter and standard deviation) were modified. The updated emission parameters and their base case values are listed in Table 3. Anthropogenic emissions of coarse PM, as well as sea spray and windblown dust, were unchanged.

The change in particle size distribution for SO_4^{2-} and Na^+ at the three BRACE sites when implementing the PM emissions adjustment is shown in Fig. 10. Particle size distributions are narrower and shifted toward smaller sizes in the PMEMIS simulation compared to the BASE simulation, in better agreement with the observations. This model change affects only the fine mode peak (e.g. SO_4^{2-}) and does not impact the coarse mode peak (e.g. Na^+). Overall, changing the input PM emissions distribution improves CMAQ estimated inorganic particle size distributions compared to the observations.

5.2 Constrained mode widths

CMAQ uses three lognormal modes to model the aerosol size distribution, where each mode is characterized by three parameters: particle number, geometric mean diameter, and geometric standard deviation (Binkowski and Roselle, 2003). Though the mode standard deviations (widths) are calculated as prognostic variables within the aerosol code, they are constrained between the values 1.05 and 2.50. Furthermore, due to numerical instabilities the coarse mode width is not allowed to vary during condensation and evaporation (Kelly et al., 2010). CMAQ mode widths often reach the allowed upper bound, which reduces confidence that they are being simulated accurately. Several other state-of-the-science modal aerosol models use fixed mode widths, e.g., COSMO-ART (Vogel et al., 2009) and MESSy/MADE3 (Kaiser et al., 2014), though other models also allow mode widths to vary (e.g., RAQM2/MADMS; Kajino et al., 2012). To explore how using fixed mode widths might affect CMAQ simulated size distributions, a model sensitivity study “CONSIG” based on the PMEMIS simulation was conducted in which the modal standard deviation constraints were modified from 1.05–2.50 to ±0.1 from their emitted values, i.e., the Aitken mode and accumulation mode standard deviations were constrained between 1.6 and 1.8, while the coarse mode standard deviation was constrained between 2.1 and 2.3.

The difference in particle size distribution between the PMEMIS simulation and the CONSIG simulation is also shown in Fig. 10. ~~Similar to the PMEMIS sensitivity, constraining the~~ Constraining the mode widths tends to produce an accumulation mode peak that is narrower and shifted to smaller sizes than the PMEMIS simulation, resulting in a better comparison against the observations. For the coarse mode however, constraining the mode widths results in a wider and lower peak than the PMEMIS simulations, which does not compare as well to the observations. Of course, the impact on model performance is directly dependent on the values chosen to constrain the particle mode widths, and alternative constraints could potentially improve performance for the coarse mode. These results do suggest, however, that the modeled size distribution is sensitive to the treatment of the mode widths, and that improvements in the algorithm that computes them would be beneficial.

5.3 Gravitational settling

Although the CMAQ aerosol module simulates gravitational settling for particles in the lowest model layer in computing their dry deposition velocities (Binkowski and Roselle, 2003), a potential limitation of the approach is the absence of gravitational settling for particles above layer 1. As a result, coarse particles emitted or convectively mixed above the first model layer can artificially remain aloft and be transported downwind farther than is realistic. As part of the development for CMAQ v5.1, a gravitational settling scheme has been implemented in which settling velocities are calculated for accumulation and coarse mode aerosol zeroth, second, and third moments in each grid cell. The method is a Stokes law approach using the same equations used in computing aerosol deposition velocities to the surface in layer 1 (see Eq. A31–A32 in Binkowski and Shankar, 1995). The settling velocities are then used in a sedimentation sub-module to calculate the moment fluxes through model layers using a first-order upstream relation.

The difference in average Na^+ size distributions simulated with and without gravitational settling is shown in Fig. 11. Because the impact of gravitational settling is significant only for larger particles, there is no discernible effect on the fine-mode range of the aerosol size distribution when gravitational settling is included. However, there is a substantial increase in the coarse-mode size range. The coarse mode peak is higher at the coastal BRACE sites in the GRAV simulation due to particles settling from upper model layers into the lowest model layer, increasing the overall surface layer concentration. The impact of gravitational settling is much less significant for inland locations that are not as impacted by sea spray. Including the effects of gravitational settling has only a very minor impact on modeled $PM_{2.5}$ mass.

6 Summary and conclusions

Size resolved particle ion SO_4^{2-}, NO_3^-, NH_4^+, Cl^-, Na^+, Mg^{2+}, Ca^{2+} and K^+ measurements for sites located throughout the United States and Canada in 2002–2005 were compared to CMAQv5.0.1 model output to assess the ability of the model to reproduce the observed particle mass size distribution. A total of 24 different measurement campaigns (some sites measured in two different seasons) were available across the four years. The model was generally able to reproduce the observed SO_4^{2-} and NH_4^+ distributions at most of the sites, but tended to overestimate the peak diameter and underestimate the peak particle concentration. NH_4^+ was substantially underestimated at the SGO site, likely due to underestimated NH_3 emissions in California's South Coast Air Basin.

CMAQ was generally able to capture the size distribution and higher concentrations of Na^+ and Cl^- at coastal and near-coastal sites. The model also reasonably captures Mg^{2+} concentrations and size distributions for those sites where Mg^{2+} originates from sea spray (e.g., the three BRACE sites in Florida), but underpredicts at sites influenced by soil dust, particularly in the western portion of the modeling domain. By contrast, the model substantially underpredicts Ca^{2+} at many coastal sites while having better performance than for Mg^{2+} at some inland sites, which may be attributable to errors in windblown dust emissions as well as speciation profiles for ~~various source categories, including~~ windblown and anthropogenic fugitive dust. K^+, which has contributions from residential wood combustion and wildfires as well as sea spray, exhibits somewhat better model performance than Ca^{2+}. Model performance for NO_3^- was mixed, with good performance at some sites (e.g., BRL, CHA1, KEJ1, and LED2), overpredicted concentrations in the accumulation mode size range at some sites (e.g., BRG, FRS, and SPR2), and substantially underestimated accumulation mode NO_3^- at SGO1 and underestimated coarse particle concentrations at other sites (e.g., GRC, GSM, and YOS).

An examination of the difference in model performance between calculating $PM_{2.5}$ mass from the modeled size distribution or by summing the masses in the Aitken and accumulation modes (PM_{ij}) shows that using the size distribution parameters results in values which on average are smaller by 0.3–1.2 $\mu g\,m^{-3}$. On a daily basis, the difference between $PM_{2.5}$ and PM_{ij} is usually less than 1 $\mu g\,m^{-3}$, regardless of season or year. The largest differences between $PM_{2.5}$ and PM_{ij} occur in the eastern US during the summer. Concentrations of SO_4^{2-} are much higher in the eastern US than in the west. Higher humidities in the eastern US, together with the high hygroscopicity of SO_4^{2-}, lead to growth of the accumulation mode beyond the 2.5 µm size range.

For operational model evaluation, the difference in aggregated model performance between the two methods in comparison to observations is generally very small. Regional scale assessments based on determination of relative response factors (RRFs), such as development of State Implementation Plans, would likely be unaffected by the choice of using $PM_{2.5}$ or PM_{ij}. For studies that involve absolute contributions of PM, particularly at the fine scale, the difference between $PM_{2.5}$ and PM_{ij} may warrant further consideration. The dataset used here, consisting of observations at mostly rural locations and limited to inorganic components of PM, as well as modeling conducted using relatively coarse 36 km grid cells, does not allow us to conclude which approach is more accurate in all cases. In urban areas dominated by primary emissions, PM_{ij} may be preferable to ensure consistency with emission inventories, as the $PM_{2.5}$ approach would immediately apportion some fraction of primary emissions to being outside the 2.5 µm size range. In remote or western regions, however, where PM is highly aged or dust is a main contributor, $PM_{2.5}$ may be preferable to account for growth outside the 2.5 µm size range or the sub-2.5 µm shoulder of the coarse mode.

Two updates to the aerosol model that are scheduled for the next release of CMAQ were evaluated. Increasing the fraction of primary PM emissions apportioned to the Aitken mode from 0.1 to 10 % and modifying the geometric mean diameter and standard deviation of the emitted particles, as recommended by Elleman and Covert (2010), caused the peak diameter of the accumulation mode to decrease, in better agreement with the observations. Implementing gravitational settling for the accumulation and coarse modes for layers above the lowest model layer led to an increase in coarse mode Na^+ from sea spray near the coast. Finally, an experiment in which the mode standard deviations were constrained to a relatively narrow range led to further reduction of accumulation mode peak diameters. Given the sensitivity of the size distribution to the treatment of mode standard deviations, future work should focus on determining the best approach for representing these variables in the model.

It is important to note that this evaluation of the CMAQ modeled aerosol size distributions has focused on the mass size distribution and has considered only inorganic species. As understanding of the health impacts associated with particular PM components and size ranges develops (e.g., Delfino et al., 2011), evaluating predictions of carbonaceous and ultrafine particle size distributions in urban environments could be valuable to support health and exposure applications. Similarly, as the state of the science evolves toward more frequent use of the two-way coupled WRF-CMAQ model (Wong et al., 2012) to capture the influence of air pollution on atmospheric dynamics, particularly the effect on clouds (Yu et al., 2014) it will be important to evaluate modeled aerosol number and surface area distributions as well.

Code availability

CMAQ model documentation and released versions of the source code are available at www.cmaq-model.org. The updates described here, as well as model postprocessing scripts, are available upon request.

The Supplement related to this article is available online at doi:10.5194/gmdd-0-1-2015-supplement.

Acknowledgements. We thank Taehyoung Lee (Colorado State University), Noreen Poor (University of South Florida), and Charles Stanier (University of Iowa) for providing MOUDI measurements that helped make this analysis possible. Brett Gantt and Rohit Mathur (US EPA) provided constructive comments in reviewing this manuscript. We thank Heather Simon and George Pouliot (US EPA) for their assistance with PM profiles in the SPECIATE database. The United States Environmental Protection Agency through its Office of Research and Development supported the research described

here. It has been subjected to Agency review and approved for publication. The views and interpretations in this publication are those of the authors and are not necessarily attributable to their organizations.

References

Allen, D. J., Pickering, K. E., Pinder, R. W., Henderson, B. H., Appel, K. W., and Prados, A.: Impact of lightning-NO on eastern United States photochemistry during the summer of 2006 as determined using the CMAQ model, Atmos. Chem. Phys., 12, 1737–1758, doi:10.5194/acp-12-1737-2012, 2012.

Appel, K. W., Bhave, P. V., Gilliland, A. B., Sarwar, G., and Roselle, S. J.: Evaluation of the Community Multiscale Air Quality (CMAQ) model version 4.5: sensitivities impacting model performance; Part II – Particulate matter, Atmos. Environ., 42, 6057–6066, doi:10.1016/j.atmosenv.2008.03.036, 2008.

Appel, K. W., Pouliot, G. A., Simon, H., Sarwar, G., Pye, H. O. T., Napelenok, S. L., Akhtar, F., and Roselle, S. J.: Evaluation of dust and trace metal estimates from the Community Multiscale Air Quality (CMAQ) model version 5.0, Geosci. Model Dev., 6, 883–899, doi:10.5194/gmd-6-883-2013, 2013.

Asgharian, B., Hofmann, W., and Bergmann, R.: Particle deposition in a multiple-path model of the human lung, Aerosol Sci. Tech., 34, 332–339, 2001.

Baker, K. R. and Foley, K. M.: A nonlinear regression model estimating single source concentrations of primary and secondarily formed $PM_{2.5}$, Atmos. Environ., 45, 3758–3767, doi:10.1016/j.atmosenv.2011.03.074, 2011.

Bash, J. O., Cooter, E. J., Dennis, R. L., Walker, J. T., and Pleim, J. E.: Evaluation of a regional air-quality model with bidirectional NH_3 exchange coupled to an agroecosystem model, Biogeosciences, 10, 1635–1645, doi:10.5194/bg-10-1635-2013, 2013.

Bey, I., Jacob, D. J., Yantosca, R. M., Logan, J. A., Field, B. D., Fiore, A. M., Li, Q., Liu, H. Y., Mickley, L. J., and Schulz, M. G.: Global modeling of tropospheric chemistry with assimilated meteorology: model description and evaluation, J. Geophys. Res., 106, 23073–23095, doi:10.1029/2001JD000807, 2001.

Binkowski, F. S. and Roselle, S. J.: Models-3 Community Multiscale Air Quality (CMAQ) model aerosol component. 1. Model description, J. Geophys. Res., 108, 4183–4201, 2003.

Binkowski, F. S. and Shankar, U.: The Regional Particulate Matter Model 1. Model description and preliminary results, J. Geophys. Res., 100, 26191–26209, 1995.

Cabada, J. C., Rees, S., Takahama, S., Khlystov, A., Pandis, S. N., Davidson, C. I., and Robinson, A. L.: Mass size distributions and size resolved chemical composition of fine particulate matter at the Pittsburgh supersite, Atmos. Environ., 38, 3127–3141, doi:10.1016/j.atmosenv.2004.03.004, 2004.

Carlton, A. G., Bhave, P. V., Napelenok, S. L., Edney, E. O., Sarwar, G., Pinder, R. W., Pouliot, G. A., and Houyoux, M.: Model representation of secondary organic aerosol in CMAQv4.7, Environ. Sci. Technol., 44, 8553–8560, doi:10.1021/es100636q, 2010.

Cooter, E. J., Bash, J. O., Benson, V., and Ran, L.: Linking agricultural crop management and air quality models for regional to national-scale nitrogen assessments, Biogeosciences, 9, 4023–4035, doi:10.5194/bg-9-4023-2012, 2012.

Delfino, R. J., Staimer, N., and Vaziri, N. D.: Air pollution and circulating biomarkers of oxidative stress, Air Qual. Atmos. Health, 4, 37–52, doi:10.1007/s11869-010-0095-2, 2011.

Elleman, R. A. and Covert, D. S.: Aerosol size distribution modeling with the Community Multiscale Air Quality modeling system in the Pacific northwest: 3. Size distribution of particles emitted into a mesoscale model, J. Geophys. Res., 115, D03204, doi:10.1029/2009JD012401, 2010.

Evans, M. C., Campbell, S. W., Bhethanabotla, V., and Poor, N. D.: Effect of sea salt and calcium carbonate interactions with nitric acid on the direct dry deposition of nitrogen to Tampa Bay, Florida, Atmos. Environ., 38, 4847–4858, 2004.

Foley, K. M., Roselle, S. J., Appel, K. W., Bhave, P. V., Pleim, J. E., Otte, T. L., Mathur, R., Sarwar, G., Young, J. O., Gilliam, R. C., Nolte, C. G., Kelly, J. T., Gilliland, A. B., and Bash, J. O.: Incremental testing of the Community Multiscale Air Quality (CMAQ) modeling system version 4.7, Geosci. Model Dev., 3, 205–226, doi:10.5194/gmd-3-205-2010, 2010.

Fountoukis, C. and Nenes, A.: ISORROPIA II: a computationally efficient thermodynamic equilibrium model for K^+-Ca^{2+}-Mg^{2+}-NH_4^+-Na^+-SO_4^{2-}-NO_3^--Cl^--H_2O aerosols, Atmos. Chem. Phys., 7, 4639–4659, doi:10.5194/acp-7-4639-2007, 2007.

Frank, N. H.: Retained Nitrate, Hydrated Sulfates, and Carbonaceous Mass in Federal Reference Method Fine Particulate Matter for Six Eastern U.S. Cities, J. Air Waste Manage. Assoc., 56, 500–511, 2006.

Henderson, B. H., Akhtar, F., Pye, H. O. T., Napelenok, S. L., and Hutzell, W. T.: A database and tool for boundary conditions for regional air quality modeling: description and evaluation, Geosci. Model Dev., 7, 339–360, doi:10.5194/gmd-7-339-2014, 2014.

Herner, J. D., Aw, J., Gao, O., Chang, D. P., and Kleeman, M. J.: Size and composition distribution of airborne particulate mattern in northern California: I – Particulate mass, carbon, and water-soluble ions, J. Air Waste Manage., 55, 30–51, doi:10.1080/10473289.2005.10464600, 2005.

Houyoux, M. R., Vukovich, J. M., Coats Jr., C. J., Wheeler, N. J. M., and Kasibhatla, P. S.: Emission inventory development and processing for the Seasonal Model for Regional Air Quality (SMRAQ) project, J. Geophys. Res., 105, 9079–9090, 2000.

Jiang, W., Smyth, S., Giroux, É., Roth, H., and Yin, D.: Differences between CMAQ fine mode particle and $PM_{2.5}$ concentrations and their impact on model performance evaluation in the lower Fraser Valley, Atmos. Environ., 40, 4973–4985, doi:10.1016/j.atmosenv.2005.10.069, 2006.

Kain, J. S.: The Kain–Fritsch convective parameterization: an update, J. Appl. Meteorol., 43, 170–181, doi:10.1175/1520-0450(2004)043<0170:TKCPAU>2.0.CO;2, 2004.

Kaiser, J. C., Hendricks, J., Righi, M., Riemer, N., Zaveri, R. A., Metzger, S., and Aquila, V.: The MESSy aerosol submodel MADE3 (v2.0b): description and a box model test, Geosci. Model Dev., 7, 1137–1157, doi:10.5194/gmd-7-1137-2014, 2014.

Kajino, M., Inomata, Y., Sato, K., Ueda, H., Han, Z., An, J., Katata, G., Deushi, M., Maki, T., Oshima, N., Kurokawa, J., Ohara, T., Takami, A., and Hatakeyama, S.: Development of the RAQM2 aerosol chemical transport model and predictions of the Northeast Asian aerosol mass, size, chemistry, and mixing type, Atmos. Chem. Phys., 12, 11833–11856, doi:10.5194/acp-12-11833-2012, 2012.

Kelly, J. T., Bhave, P. V., Nolte, C. G., Shankar, U., and Foley, K. M.: Simulating emission and chemical evolution of coarse sea-salt particles in the Community Multiscale Air Quality (CMAQ) model, Geosci. Model Dev., 3, 257–273, doi:10.5194/gmd-3-257-2010, 2010.

Kelly, J. T., Avise, J., Cai, C., and Kaduwela, A. P.: Simulating particle size distributions over California and impact on lung deposition fraction, Aerosol Sci. Tech., 45, 148–162, doi:10.1080/02786826.2010.528078, 2011.

Kelly, J. T., Baker, K. R., Nowak, J. B., Murphy, J. G., Markovic, M. Z., VandenBoer, T. C., Ellis, R. A., Neuman, J. A., Weber, R. J., Roberts, J. M., Veres, P. R., de Gouw, J. A., Beaver, M. R., Newman, S., and Misenis, C.: Fine-scale simulation of ammonium and nitrate over the South Coast Air Basin and San Joaquin Valley of California during CalNex-2010, J. Geophys. Res., 119, 3600–3614, doi:10.1002/2013JD021290, 2014.

Lee, T.: Characterizing ionic components of aerosol in rural environments: temporal variability, size distributions, and the form of particle nitrate, Ph.D. thesis, Colorado State University, 2007.

Lee, T., Yu, X.-Y., Ayres, B., Kreidenweis, S. M., Malm, W. C., and Collett Jr., J. L.: Observations of fine and coarse particle nitrate at several rural locations in the United States, Atmos. Environ., 42, 2720–2732, doi:10.1016/j.atmosenv.2007.05.016, 2008a.

Lee, T., Yu, X.-Y., Kreidenweis, S. M., Malm, W. C., and Collett Jr., J. L.: Semi-continuous measurement of $PM_{2.5}$ ionic composition at several rural locations in the United States, Atmos. Environ., 42, 6655–6669, doi:10.1016/j.atmosenv.2008.04.023, 2008b.

Malm, W. C., Day, D. E., Carrico, C., Kreidenweis, S. M., Collett Jr., J. L., McMeeking, G., Lee, T., Carillo, J., and Schichtel, B.: Intercomparison and closure calculations using measurements of aerosol species and optical properties during the Yosemite Aerosol Characterization Study, J. Geophys. Res., 110, D14302, doi:10.1029/2004JD005494, 2005.

Marple, V. A., Rubow, K. L., and Behm, S. M.: A Microorifice Uniform Deposit Impactor (MOUDI): description, calibration, and use, Aerosol Sci. Tech., 14, 434–446, doi:10.1080/02786829108959504, 1991.

Morrison, H., Thompson, G., and Tatarskii, V.: Impact of cloud microphysics on the development of trailing stratiform precipitation in a simulated squall line: comparison of one- and two-moment schemes, Mon. Weather Rev., 137, 991–1007, doi:10.1175/2008MWR2556.1, 2009.

Nolte, C. G., Bhave, P. V., Arnold, J. R., Dennis, R. L., Zhang, K. M., and Wexler, A. S.: Modeling urban and regional aerosols–Application of the CMAQ-UCD aerosol model to Tampa, a coastal urban site, Atmos. Environ., 42, 3179–3191, doi:10.1016/j.atmosenv.2007.12.059, 2008.

Nowak, J. B., Neuman, J. A., Bahreini, R., Middlebrook, A. M., Holloway, J. S., McKeen, S. A., Parrish, D. D., Ryerson, T. B., and Trainer, M.: Ammonia sources in the California South Coast Air Basin and their impact on ammonium nitrate formation, Geophys. Res. Lett., 39, L07804, doi:10.1029/2012GL051197, 2012.

Otte, T. L. and Pleim, J. E.: The Meteorology-Chemistry Interface Processor (MCIP) for the CMAQ modeling system: updates through MCIPv3.4.1, Geosci. Model Dev., 3, 243–256, doi:10.5194/gmd-3-243-2010, 2010.

Pleim, J. E.: A combined local and non-local closure model for the atmospheric boundary layer. Part 1: Model description and testing, J. Appl. Meteorol. Clim., 46, 1383–1395, doi:10.1175/JAM2539.1, 2007a.

Pleim, J. E.: A combined local and non-local closure model for the atmospheric boundary layer. Part 2: Application and evaluation in a mesoscale model, J. Appl. Meteorol. Clim., 46, 1396–1409, doi:10.1175/JAM2534.1, 2007b.

Pleim, J. E. and Xiu, A.: Development and testing of a surface flux and planetary boundary model for application in mesoscale models, J. Appl. Meteorol., 34, 16–32, doi:10.1175/1520-0450-34.1.16, 1995.

Raffuse, S. M., Pryden, D. A., Sullivan, D. C., Larkin, N. K., Strand, T., and Solomon, R.: SMARTFIRE algorithm description, Sonoma Technol., Inc., Petaluma, Calif., available at: http://firesmoke.ca/smartfire/pdfs/SMARTFIRE_Algorithm_Description_Final.pdf (last access: 12 May 2015), 2009.

Reff, A., Bhave, P. V., Simon, H., Pace, T. G., Pouliot, G. A., Mobley, J. D., and Houyoux, M.: Emissions inventory of $PM_{2.5}$ trace elements across the United States, Environ. Sci. Technol., 43, 5790–5796, doi:10.1021/es802930x, 2009.

Sarwar, G., Appel, K. W., Carlton, A. G., Mathur, R., Schere, K., Zhang, R., and Majeed, M. A.: Impact of a new condensed toluene mechanism on air quality model predictions in the US, Geosci. Model Dev., 4, 183–193, doi:10.5194/gmd-4-183-2011, 2011.

Scheffe, R. D., Lynch, J. A., Reff, A., Kelly, J. T., Hubbell, B., Greaver, T. L., and Smith, J. T.: The Aquatic Acidification Index: a new regulatory metric linking atmospheric and biogeochemical models to assess potential aquatic ecosystem recovery, Water Air Soil Poll., 225, 1838, doi:10.1007/s11270-013-1838-0, 2014.

Simon, H., Beck, L., Bhave, P. V., Divita, F., Hsu, Y., Luecken, D., Mobley, J. D., Pouliot, G. A., Reff, A., Sarwar, G., and Strum, M.: The development and uses of EPA's SPECIATE database, Atmos. Poll. Res., 1, 196–206, doi:10.5094/APR.2010.026, 2010.

Simon, H., Baker, K. R., and Phillips, S.: Compilation and interpretation of photochemical model performance statistics published between 2006 and 2012, Atmos. Environ., 61, 124–139, doi:10.1016/j.atmosenv.2012.07.012, 2012.

Simon, H. and Bhave, P. V.: Simulating the Degree of Oxidation in Atmospheric Organic Particles, Environ. Sci. Technol., 46, 331–339, doi:10.1021/es202361w, 2012.

Skamarock, W. C. and Klemp, J. B.: A time-split nonhydrostatic atmospheric model for weather research and forecasting applications, J. Comput. Phys., 227, 3465–3485, doi:10.1016/j.jcp.2007.01.037, 2008.

Stanier, C. O., Khlystov, A. Y., and Pandis, S. N.: Ambient aerosol size distributions and number concentrations measured during the Pittsburgh Air Quality Study (PAQS), Atmos. Environ., 38, 3275–3284, doi:10.1016/j.atmosenv.2004.03.020, 2004.

Vogel, B., Vogel, H., Bäumer, D., Bangert, M., Lundgren, K., Rinke, R., and Stanelle, T.: The comprehensive model system COSMO-ART – Radiative impact of aerosol on the state of the atmosphere on the regional scale, Atmos. Chem. Phys., 9, 8661–8680, doi:10.5194/acp-9-8661-2009, 2009.

Vukovich, J. M. and Pierce, T.: The implementation of BEIS3 within the SMOKE modeling framework, in: Proceedings of the 11th International Emissions Inventory Conference, Atlanta, Georgia, available at: http://www.epa.gov/ttn/chief/conference/ei11/modeling/vukovich.pdf (last access: 11 May 2015), 2002.

Wong, D. C., Pleim, J., Mathur, R., Binkowski, F., Otte, T., Gilliam, R., Pouliot, G., Xiu, A., Young, J. O., and Kang, D.: WRF-CMAQ two-way coupled system with aerosol feedback: software development and preliminary results, Geosci. Model Dev., 5, 299–312, doi:10.5194/gmd-5-299-2012, 2012.

Yao, X. and Zhang, L.: Chemical processes in sea-salt chloride depletion observed at a Canadian rural coastal site, Atmos. Environ., 46, 189–194, doi:10.1016/j.atmosenv.2011.09.081, 2012.

Yu, S., Dennis, R., Roselle, S., Nenes, A., Walker, J., Eder, B., Schere, K., Swall, J., and Roberge, W.: An assessment of the ability of three-dimensional air quality models with current thermodynamic equilibrium models to predict aerosol NO_3, J. Geophys. Res., 110, doi:10.1029/2004JD004718, 2005.

Yu, S., Mathur, R., Pleim, J., Wong, D., Gilliam, R., Alapaty, K., Zhao, C., and Liu, X.: Aerosol indirect effect on the grid-scale clouds in the two-way coupled WRF–CMAQ: model description, development, evaluation and regional analysis, Atmos. Chem. Phys., 14, 11247–11285, doi:10.5194/acp-14-11247-2014, 2014.

Zhang, L., Vet, R., Wiebe, A., Mihele, C., Sukloff, B., Chan, E., Moran, M. D., and Iqbal, S.: Characterization of the size-segregated water-soluble inorganic ions at eight Canadian rural sites, Atmos. Chem. Phys., 8, 7133–7151, doi:10.5194/acp-8-7133-2008, 2008.

Zhang, Y., Liu, P., Pun, B., and Seigneur, C.: A comprehensive performance evaluation of MM5-CMAQ for the Summer 1999 Southern Oxidants Study episode – Part III: Diagnostic and mechanistic evaluations, Atmos. Environ., 40, 4856–4873, 2006.

Table 1. Summary of the MOUDI data used in this study.

Code	Location	Comment	Lat. N	Long. W	Dates	Ref.*
ALG1 ALG2	Algoma, ON	moderately polluted	47.04	84.38	8–27 Feb 2003 5–26 Jun 2003	a
AZP	Azalea Park, FL	urban coastal	27.78	82.74	4 May–2 Jun 2002	b
BON	Bondville, IL	agricultural	40.05	88.37	1–27 Feb 2003	c
BRL	Bratt's Lake, SK	polluted agricultural	50.20	104.20	11 Feb–4 Mar 2005	a
BRG	Brigantine, NJ	coastal wildlife refuge	39.46	74.45	4–30 Nov 2003	c
CHA1 CHA2	Chalk River, ON	moderately polluted	46.06	77.40	22 Jan–21 Feb 2004 4–26 Jun 2004	a
EGB	Egbert, ON	polluted agricultural	44.23	79.78	6–13 Mar 2002	a
FRS	Frelighsberg, QC	polluted rural foothills	45.05	73.06	4–16 May 2002	a
GAN	Gandy Bridge, FL	urban coastal	27.97	82.23	4 May–2 Jun 2002	b
GRC	Grand Canyon, AZ	remote	35.97	111.98	1–30 May 2003	c
GSM	Great Smokies, TN	mountainous	35.63	83.94	22 Jul–19 Aug 2004	c
KEJ1 KEJ2	Kejimkujik, NS	clean coastal	44.43	65.21	29 June–15 Jul 2002 25 Oct–15 Nov 2003	a
LED1 LED2	Lac Édouard, QC	clean continental	47.68	72.44	11–27 Aug 2003 17 Oct–3 Nov 2003	a
PIT	Pittsburgh, PA	urban	40.44	79.94	1–17 Jan 2002	d
SGO1 SGO2	San Gorgonio, CA	mountainous	34.19	116.90	4–26 May 2003 1–30 Jul 2003	c
SPR1 SPR2	Sprucedale, ON	moderately polluted	45.42	79.49	17 Aug–18 Sep 2004 16 Nov–12 Dec 2004	a
SYD	Sydney, FL	urban coastal	27.97	82.23	4 May–2 Jun 2002	b
YOS	Yosemite CA	mountainous	37.75	119.59	15 Jul–2 Sep 2004	c

* a, Zhang et al. (2008); b, Evans et al. (2004); c, Lee et al. (2008a); d, Cabada et al. (2004).

Table 2. Comparison of CMAQ PM model performance relative to observations at IMPROVE, CSN and AQS network sites during 2002 using the sum of masses in the Aitken and accumulation modes (PM_{ij}) and calculated using the modeled size distribution ($PM_{2.5}$).

	MB (µg m^{-3})			ME (µg m^{-3})			RMSE (µg m^{-3})		
Season	$PM_{2.5}$	PM_{ij}	Δ*	$PM_{2.5}$	PM_{ij}	Δ	$PM_{2.5}$	PM_{ij}	Δ
Winter (DJF)	2.38	2.42	−0.04	5.19	5.28	−0.09	8.68	8.73	−0.05
Spring (MAM)	0.46	0.53	−0.07	3.64	3.65	−0.01	6.07	6.11	−0.04
Summer (JJA)	−3.60	−3.30	−0.30	5.85	5.63	0.22	9.90	9.69	0.21
Fall (SON)	0.96	1.16	−0.20	4.77	4.79	−0.02	7.98	8.01	−0.03
Average	0.05	0.20	−0.15	4.86	4.84	0.02	8.16	8.14	0.02

* $PM_{2.5} - PM_{ij}$.

Table 3. Parameters for Aitken and accumulation mode particulate emissions for the BASE run and PMEMIS sensitivity case.

		BASE			PMEMIS		
Mode	Species	Mass Fraction	D_{gv} (µm)	σ_{g}	Mass Fraction	D_{gv} (µm)	σ_{g}
Aitken	EC/OC/NCOM Other	0.001 0.000	0.030	1.7	0.10	0.060	1.7
accumulation	EC/OC/NCOM Other	0.999 1.000	0.300	2.0	0.90	0.280	1.7

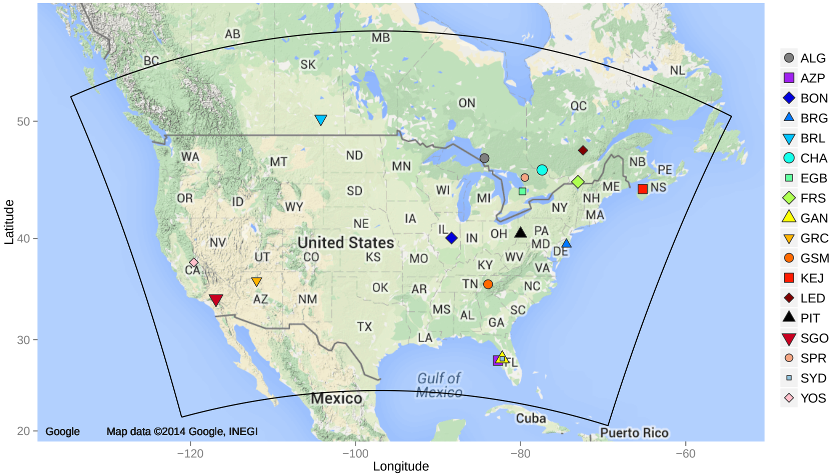

Figure 1. ~~Location~~ Locations of the sampling sites used in this study. See Table 1.

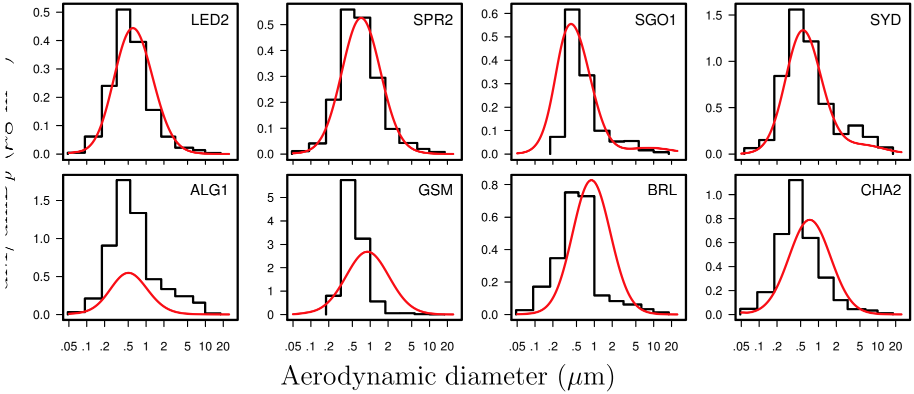

Figure 2. Average observed (black) and modeled (red) SO_4^{2-} size distributions at representative sites.

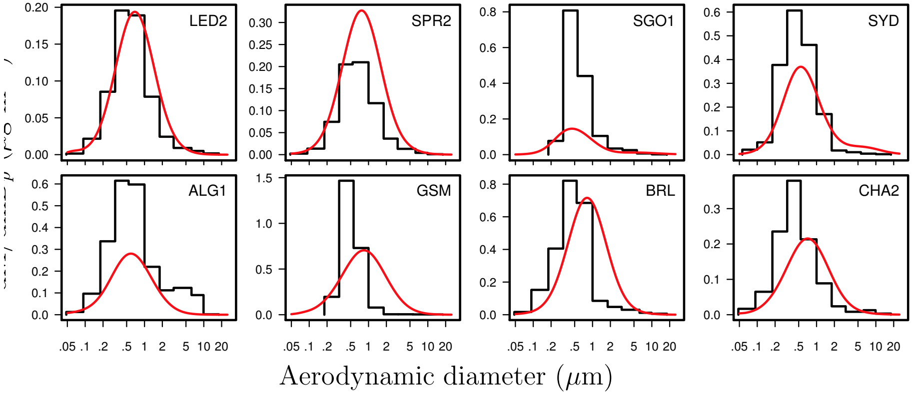

Figure 3. Average observed (black) and modeled (red) NH4^{+} size distributions at representative sites.

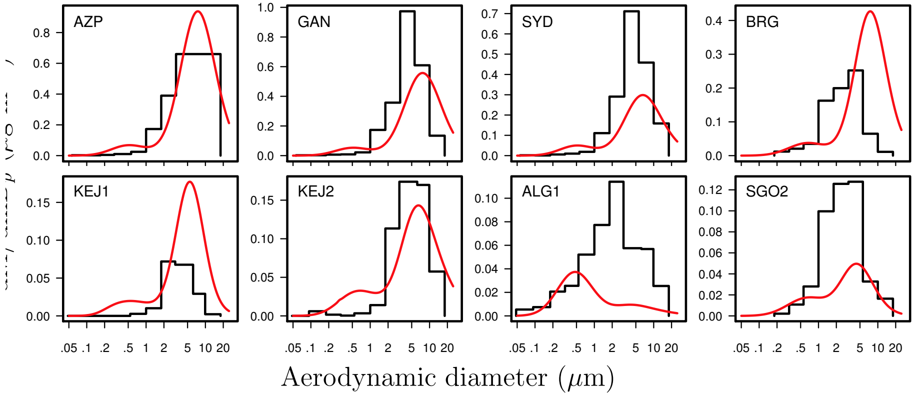

Figure 4. Average observed (black) and modeled (red) Na^+ size distributions at representative sites.

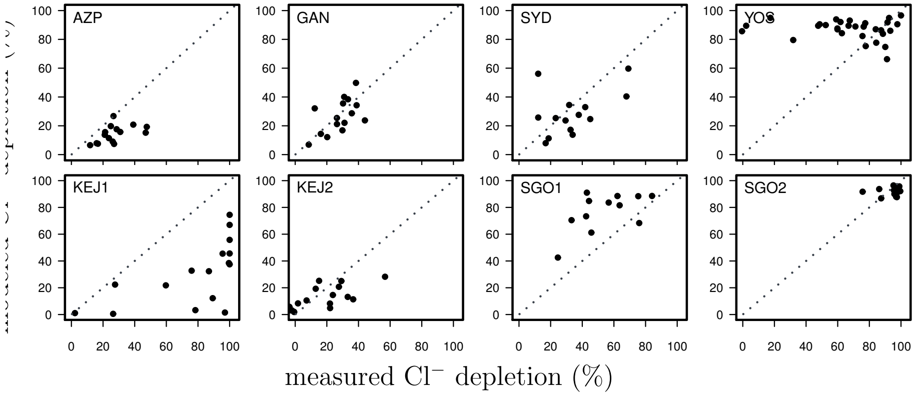

Figure 5. Scatter plots of modeled and observed chloride depletion in coarse ($D_p > 2.5\,\mu m$) particles at representative sites. Each point represents a distinct measurement period, with modeled concentrations averaged over the corresponding intervals.

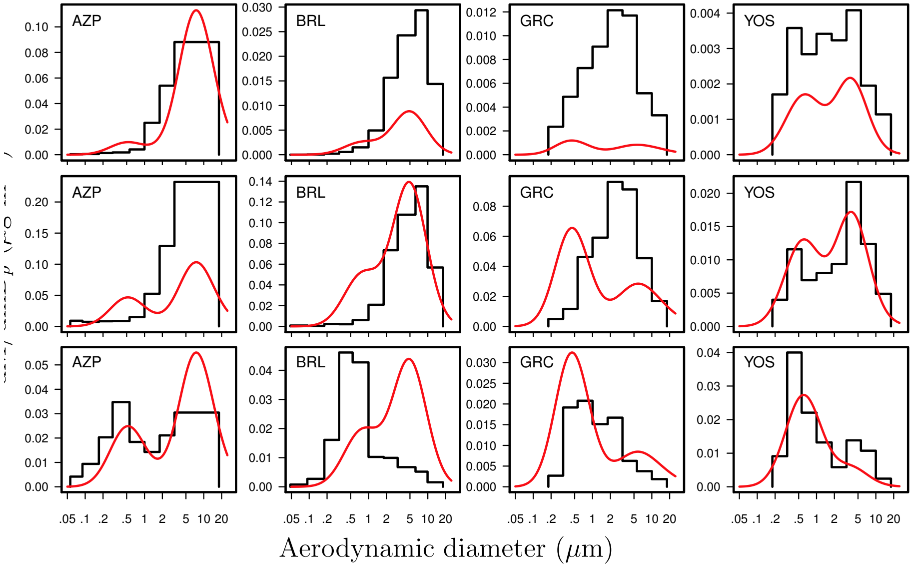

Figure 6. Average observed (black) and modeled (red) Mg^{2+} (top), Ca^{2+} (middle), and K^+ (bottom) size distributions at representative sites.

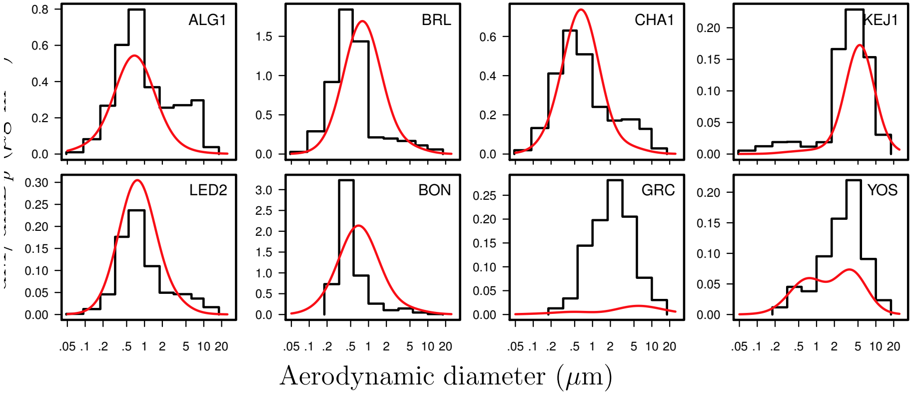

Figure 7. Average observed (black) and modeled (red) NO_3^- size distributions at representative sites.

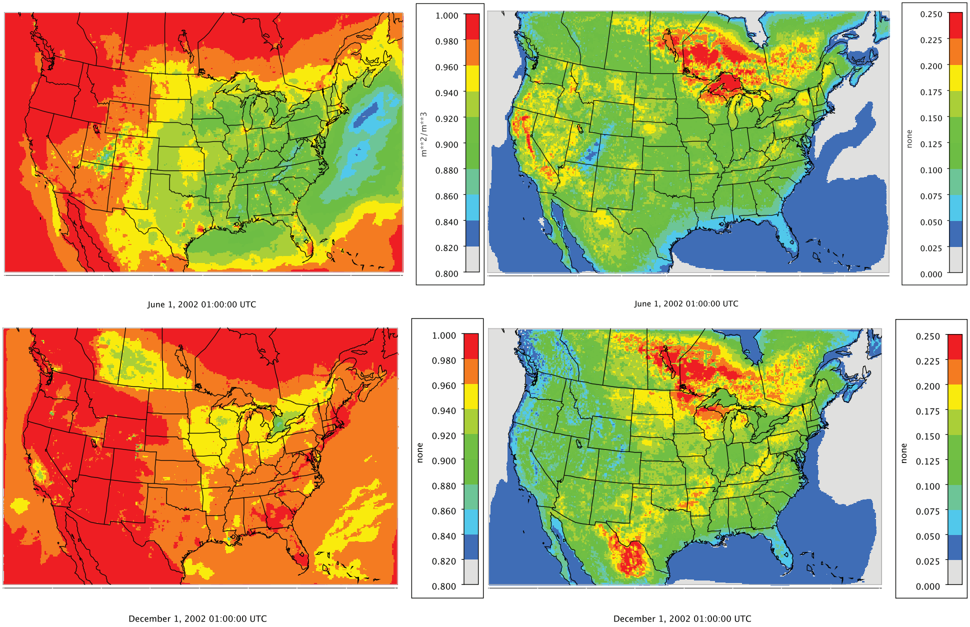

Figure 8. Fraction of accumulation mode (left) and coarse mode (right) smaller than 2.5 µm in diameter, averaged over summer (top) and winter (bottom) 2002.

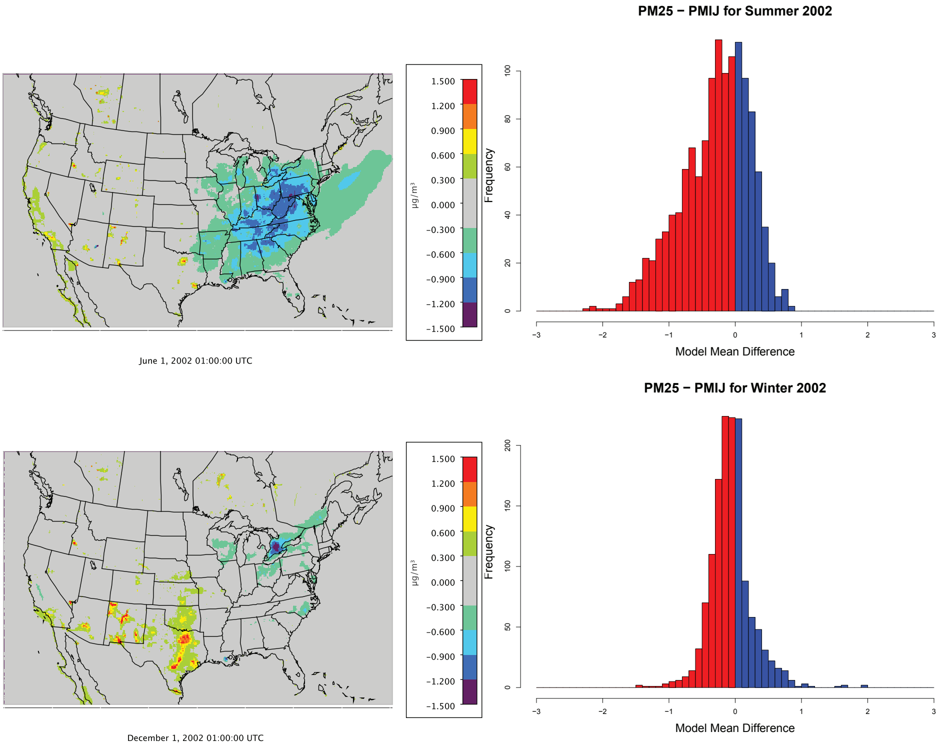

Figure 9. Difference between $PM_{2.5}$ computed using modeled size distribution and PM_{ij}, and histogram of daily average differences ($PM_{2.5} - PM_{ij}$) for summer (top) and winter (bottom) 2002. Blue shading indicates days where $PM_{2.5}$ is greater than PM_{ij}, while red shading indicates days where $PM_{2.5}$ is less than PM_{ij}.

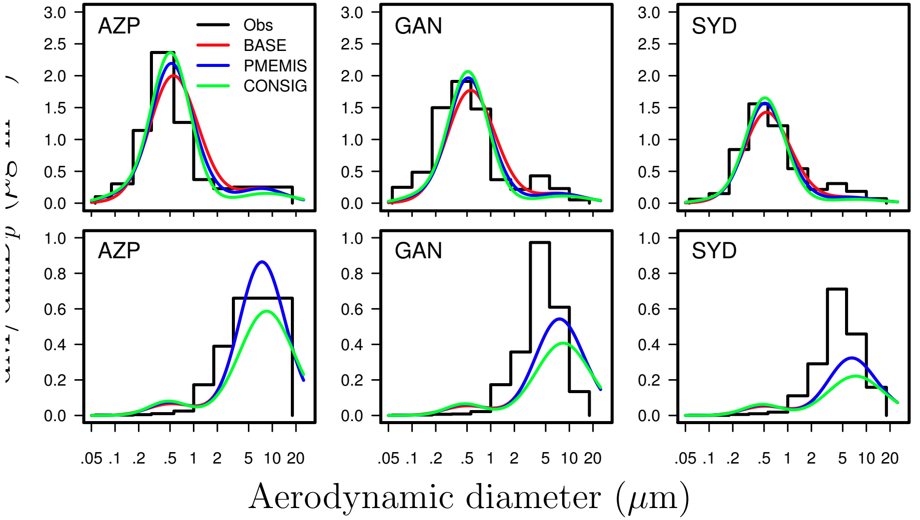

Figure 10. Observed and modeled SO_4^{2-} (top) and Na^+ (bottom) size distributions for the PMEMIS and CONSIG sensitivity simulations.

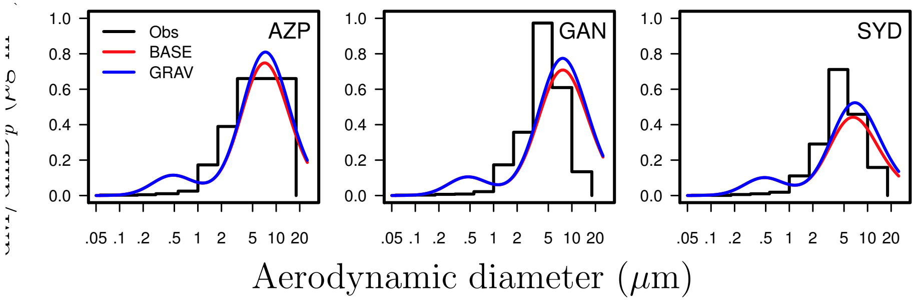

Figure 11. Observed and modeled Na^+ size distributions for the GRAV sensitivity simulation.